Raytheon

NET HEAT FLUX

VISIBLE/INFRARED IMAGER/RADIOMETER SUITE ALGORITHM THEORETICAL BASIS DOCUMENT

Version 5.1: July 2002

Corinne Carter
Quanhua Liu
Wenli Yang
Dorlisa Hommel

William Emery, Science Team Member
University of Colorado

RAYTHEON SYSTEMS COMPANY
Information Technology and Scientific Services
4400 Forbes Boulevard
Lanham, MD 20706

SBRS Document #: Y2407-NetHeatFlux-ATBD-Rev5.1

EDR: Net Heat Flux (40.7.5)

Doc No: Y2407
Version: 5
Revision: 1

	FUNCTION	NAME	SIGNATURE	DATE
Prepared By	EDR Developer	C. Carter		17 July 2002
Approved By	Relevant Lead	D. HOMMEL		17 July 2002
Approved By	Chief Scientist	S. MILLER		17 July 2002
Released By	Algorithm IPT Lead	P. KEALY		17 July 2002

TABLE OF CONTENTS

LIST OF FIGURES

LIST OF TABLES

GLOSSARY OF ACRONYMS

6S	Second Simulation of the Satellite Signal in the Solar Spectrum
ATBD	Algorithm Theoretical Basis Document
AVHRR	Advanced Very High Resolution Radiometer
BSRN	Baseline Surface Radiation Network
CERES	Clouds and the Earth's Radiation Energy System
CMIS	Conical scanning Microwave Imager/Sounder
COARE	Coupled Ocean-Atmosphere Response Experiment
CrIS	Cross Track Infrared Sounder
DISORT	Discrete Ordinate Radiative Transfer
EDR	Environmental Data Record
ENSO	El Niño Southern Oscillation
ERBE	Earth Radiation Budget Experiment
IP	Intermediate Product
ISCCP	International Satellite Cloud Climatology Project
IST	Ice Surface Temperature
LOWTRAN	Low Resolution Atmospheric Radiance and Transmittance Model
MODTRAN	Moderate Resolution Atmospheric Radiance and Transmittance Model
NCAR	National Center for Atmospheric Research
NCEP	National Centers for Environmental Prediction
NHF	Net Heat Flux
NPOESS	National Polar-orbiting Operational Environmental Satellite System
SSM/I	Special Sensor Microwave/Imager
TBD	To Be Determined
TBR	To Be Reviewed
TOA	Top Of the Atmosphere
TOGA	Tropical Ocean Global Atmosphere
TOVS	TIROS-N Operational Vertical Sounder
VIIRS	Visible/Infrared Image Radiometer Suite
WCRP	World Climate Research Program

ABSTRACT

For the first time, the Net Heat Flux (NHF) Environmental Data Record (EDR) is being developed as an operational product derived from satellite measurements. NHF can be derived from the National Polar-Orbiting Operational Environmental Satellite System (NPOESS), a multisensor satellite system. Sea and ice surface temperature and shortwave radiation flux can be obtained from the Visible/Infrared Image Radiometer Suite (VIIRS). Profiles of atmospheric temperature and humidity can be derived from Cross- track Infrared Sounder (CrIS) or Conical Scanning Microwave Imager/ Sounder (CMIS) data, and sea surface wind speed can be estimated from CMIS data. The current VIIRS Sensor Requirements Document (SRD) for the Net Heat Flux EDR specifies that it need only be produced under clear- sky conditions. As a result, the Net Heat Flux EDR depends on the VIIRS cloud masking algorithm to distinguish between clear and cloudy pixels and also to mask out pixels where sun glint prevents proper shortwave retrievals.

Net heat flux consists of the sum of two radiative flux components (net shortwave and longwave radiation at the surface) and two turbulent (sensible and latent) heat flux components. Shortwave and longwave radiation can be modeled physically, but our present formulas for calculating sensible and latent heat fluxes are approximations based on observations. All four NHF components are used widely for studying the greenhouse effect, interactions between the ocean and the atmosphere, and the global water cycle. They are key parameters for developing ocean and atmospheric models.

Net heat flux, however, is neither well understood nor easy to validate due to the sparse in-situ measurements and large measurement uncertainties. Even with modern techniques and sophisticated design, it is difficult to achieve an accuracy of 5 Wm^{-2} for each NHF component. So far, VIIRS NHF algorithm results are only compared to model simulations due to a scarcity of in-situ measurements of net heat flux at ocean surfaces. According to these tests, the VIIRS threshold requirement for accuracy, but not for precision, has been achieved. Although the VIIRS NHF uncertainty is estimated at about 25 Wm^{-2}, data with this level of uncertainty are still useful for determining the bulk temperature of the sea surface, for studying ocean currents, and for ocean-atmosphere modeling, especially for climate study. Our error analysis indicates that most of the error expected in the NHF EDR is attributable to uncertainties in data from non-VIIRS instruments or in other VIIRS EDRs. VIIRS sensor calibration error and radiometric noise are expected to contribute only relatively minor amounts of uncertainty to the NHF EDR.

1.0 INTRODUCTION

1.1 PURPOSE

Net heat flux at the ocean surface is one of the key parameters governing the atmosphere-ocean interaction. (In this document, we define net heat flux as total downwelling minus total upwelling flux.) It is required for weather prediction and climate studies related to global energy and water cycles. Using suitable models, net heat flux can be used to reproduce and predict variations of the global hydrological regime and its impact on atmospheric and surface dynamics, as well as variations in regional water resources and hydrological processes in response to such environmental changes as an increase in greenhouse gas forcing. Net heat flux, which depends on atmospheric conditions, sea surface temperature and sea surface wind, is an important component of atmosphere-ocean interactions such as the El Niño Southern Oscillation (ENSO) phenomenon. Measurement of net heat flux and its components should be useful in the study of the ENSO phenomenon and also in testing hypotheses concerning the role of evaporation and atmospheric moisture in the regulation of sea surface temperatures (*e.g.,* Priestly 1966, Ramanathan and Collins 1991, Liu and Zhang 1994).

The net heat flux is composed of the exchange of latent and sensible heat between the surface and atmosphere, combined with shortwave and longwave radiation fluxes at the surface in both upward and downward directions. Each component has significance for weather prediction and for global environmental studies. Longwave radiation as measured by satellite is dependent on forcing by atmospheric greenhouse gases (e.g., CO_2 and H_2O), surface emission, and clouds (although we are only required to report NHF under clear conditions at present). Shortwave radiation depends on clouds, aerosols, and surface albedo. Sensible heat flux is directly dependent on changes in the sea surface temperature, and latent heat flux is a measurement of evaporation.

An atlas of global monthly mean heat flux at the ocean surface has been produced with a spatial resolution of 4 degrees by 5 degrees (see Figures 1-5, all based on the Oregon State CRI Global Ocean Heat Flux). The greatest longwave and sensible heat fluxes are generally found over the warm waters of the Kuroshio Current and the Gulf Stream. The sensible heat flux is maximized during cold-air outbreaks due to large humidity differences coupled with strong offshore winds (Agee and Howley, 1977). The large positive net heat flux in the tropical region is due to the large solar incident radiation there. The net heat flux in high latitudes is negative because of the low solar insolation.

Retrieval of a Net Heat Flux Environmental Data Record (EDR) from NPOESS depends on data or EDRs from many NPOESS sensors or other data sources such as NCEP reanalyses. NPOESSS instruments include the Visible/Infrared Image Radiometer Suite (VIIRS), Conical Scanning Microwave Imager/Sounder (CMIS), and Cross Track Infrared Sounder (CrIS). The methods for obtaining net heat flux described in this document require the use of different combinations of data from different sources for each component. The shortwave radiation flux at the surface is directly calculated from VIIRS radiances. The longwave net radiation flux over the oceans is calculated from VIIRS sea surface temperatures and atmospheric profiles from CrIS or NCEP. Latent and sensible heat fluxes are calculated from the sea surface wind, air temperature, sea surface temperature, and surface specific humidity, which are EDRs of VIIRS, CMIS or

CrIS, or NCEP data products. The VIIRS Cloud Mask IP is also used to screen out cloudy and sun glint-contaminated pixels. The error budget developed in this document is based on the expected accuracy and precision of these data products. The uncertainty introduced by erroneous cloud flagging is not expected to be significant over a 20 km aggregated grid cell, as cloud-contaminated pixels are usually easily distinguishable from clear pixels over the ocean during the daytime, and at night the net heat flux consists only of longwave, sensible, and latent fluxes, and is derived from surface temperature and auxiliary data.

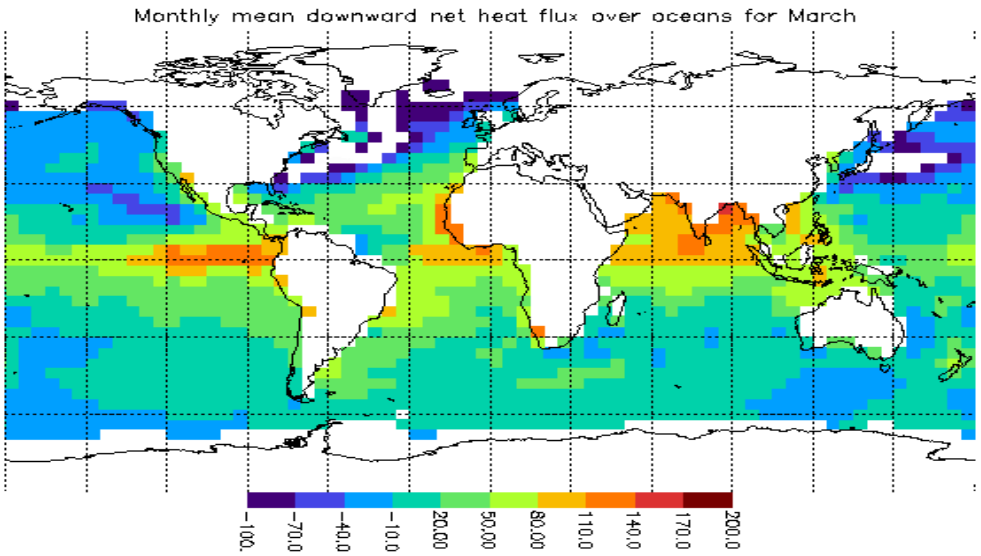

Figure 1. Monthly mean net heat flux over oceans at the surface (unit: Wm^{-2}), produced from the Oregon State CRI Global Ocean Heat Flux dataset.

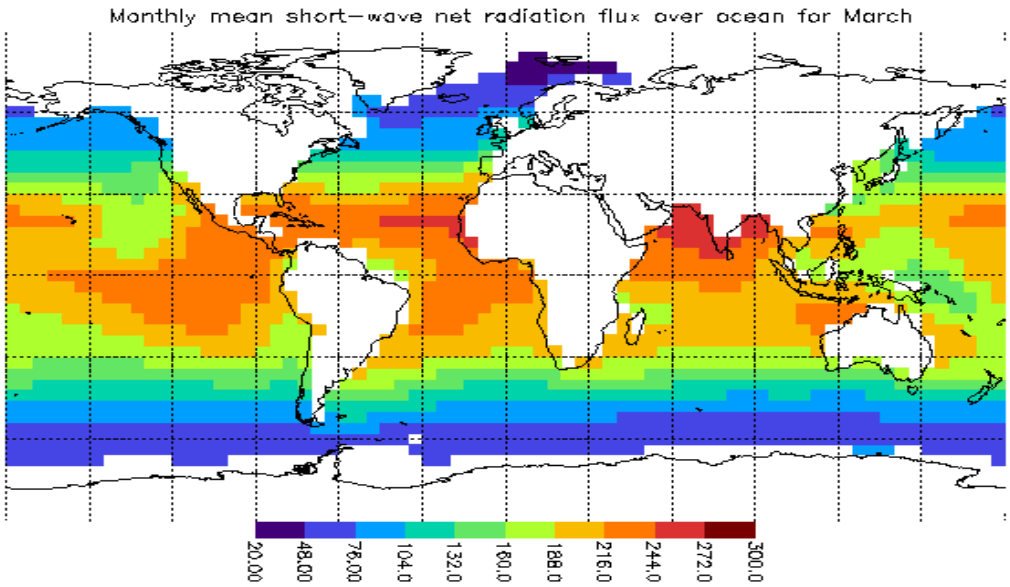

Figure 2. Monthly mean short-wave net radiation flux over oceans at the surface (unit: Wm^{-2}), produced from the Oregon State CRI Global Ocean Heat Flux dataset.

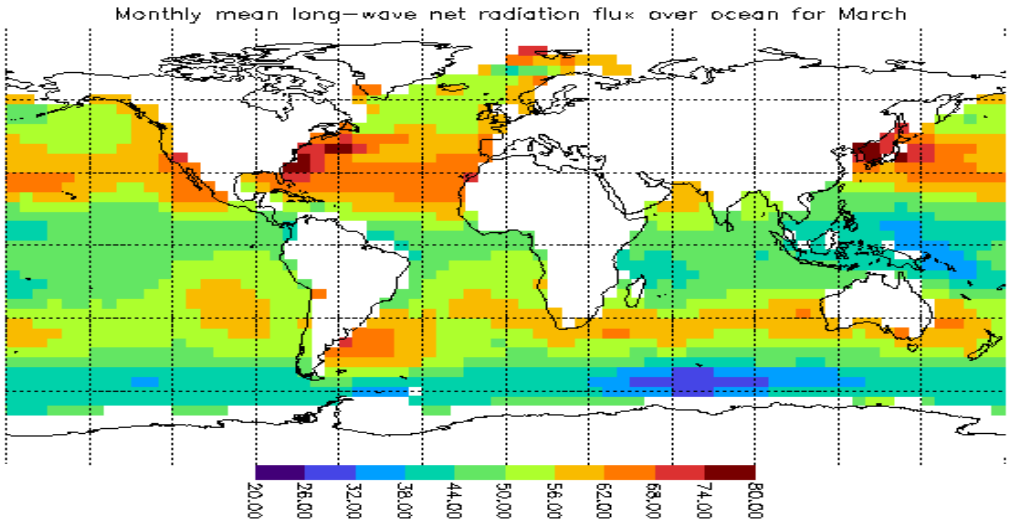

Figure 3. Monthly mean long-wave net radiation flux over oceans at the surface (unit: Wm^{-2}), produced from the Oregon State CRI Global Ocean Heat Flux dataset.

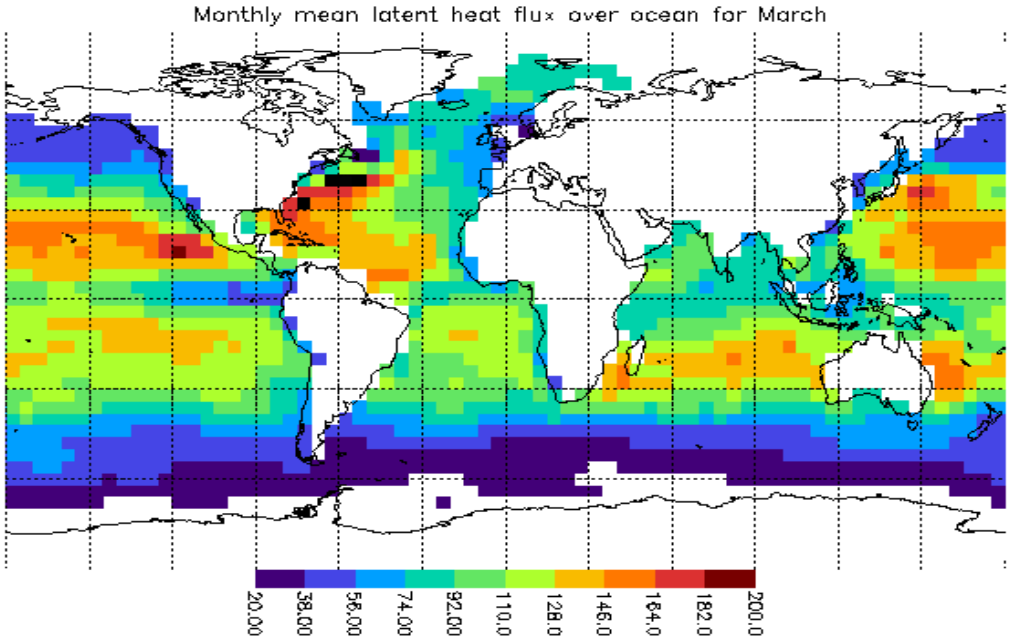

Figure 4. Monthly mean latent heat flux over oceans at the surface (unit: Wm^{-2}), produced from the Oregon State CRI Global Ocean Heat Flux dataset.

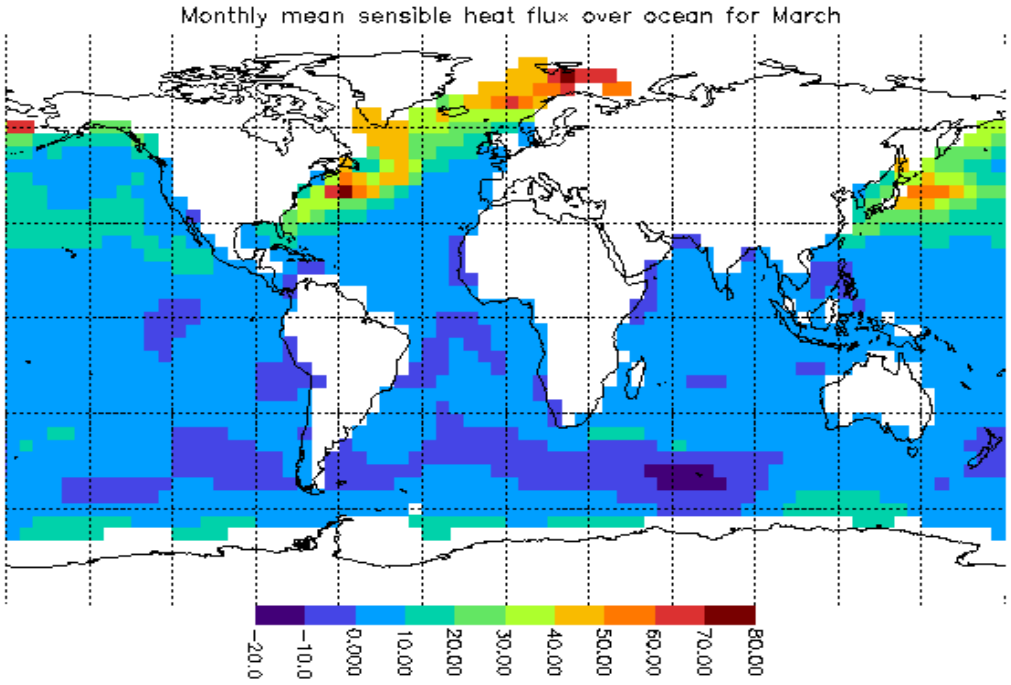

Figure 5. Monthly mean sensible heat flux over oceans at the surface (unit: Wm^{-2}), produced from the Oregon State CRI Global Ocean Heat Flux dataset.

1.2 SCOPE

This Algorithm Theoretical Basis Document (ATBD) describes the theoretical basis of the VIIRS Net Heat Flux (NHF) algorithm. Section 1 describes the purpose and scope of this document. Section 2 is an overview of previous work, present research, and future perspectives. Present and potential applications of the methods described in Section 2 to the VIIRS system are detailed in Section 3, "Algorithm Description." Section 3 also provides useful physical background, mathematical formulae, and sensitivity tests to aid in selecting significant variables and determining retrieval accuracies. A functional flowdown shows the main structure of the retrieval algorithm for each component of the net heat flux. An error analysis compares anticipated sensor and algorithm performance to VIIRS NHF EDR specifications.

1.3 VIIRS REQUIREMENTS

The National Polar-orbiting Operational Environmental Satellite System (NPOESS) science team for daily and nighttime 20 km ocean products proposed the Net Heat Flux EDR. The Net Heat Flux EDR requirements are specified by the VIIRS Sensor Requirements Document *[Y-1]*. Required at first for both clear and cloudy cases, it is currently required for clear conditions only (VIIRS Sensor Requirements Document *[Y-1]*), as the algorithm for cloudy cases is not sufficiently mature. From these requirements and information about the VIIRS instrument in development, new EDR requirements were derived by Raytheon. These derived requirements, including thresholds, objectives, and specifications, are displayed in Table 1.

Table 1. VIIRS Net Heat Flux EDR requirements.

Parameter No.		Thresholds	Objectives	Specifications
V40.7.5-1	a. Horizontal Cell Size	20 km	5 km	20 km
V40.7.5-2	b. Horizontal Reporting Interval	20 km	5 km	20 km
V40.7.5-3	c. Horizontal Coverage	Oceans	Oceans	Oceans
V40.7.5-4	d. Measurement Range	-1000 to 1000 Wm^{-2}	-2000 to 2000 Wm^{-2}	-2000 to 2000 Wm^{-2}
V40.7.5-5	e. Measurement Accuracy	10 Wm^{-2}	1 Wm^{-2}	15 Wm^{-2}
V40.7.5-6	f. Measurement Precision	5 Wm^{-2} (25)*	1 Wm^{-2} (10)*	25 Wm^{-2}
V40.7.5-7	g. Mapping Uncertainty	7 km	1 km	7 km
	h. Maximum Local Average Revisit Time	6 hours	3 hours	6 hours
	i. Maximum Local Refresh	6 hours	3 hours	6 hours
V40.7.5-8	j. Minimum Swath Width	1700 km	3000 km	1700 km
*Recommended				

1.4 REVISIONS

This Version 5, revision 1 of this document. It has been modified to incorporate substantial Navy comments. The fifth version of this document, dated March 2002, had changes are made to the text to reflect the selection of the method to be used in calculating longwave and latent heat fluxes. In both cases, VIIRS SST data will be used along with CrIS atmospheric profiles. Other changes have been made to the algorithms. The look-up table for longwave radiation will be derived from MODTRAN. CMIS wind speeds will be used in the shortwave flux algorithm to derive values for sea surface albedo. The shortwave flux can be calculated from a look-up table of MODTRAN-derived or empirical coefficients. These changes are reflected in the text and figures of Section 3.

For the fourth version of this document, dated May 2001, additions were made to the VIIRS Data section.

The third version was dated May 2000. For the third version the rationale for proposing the new EDR requirements contained in Table 1 was provided as follows: The change of the Minimum Swath Width from 3000 km to 1700 km is due to the smaller swath width of CMIS; The sea surface wind EDR from CMIS is required for calculating both the latent and sensible heat flux; Simultaneous VIIRS and CMIS measurements are required because the sea surface wind can change rapidly; the low limit of the Measurement Range is extended to –1000 (Threshold) and –2000 Wm^{-2} (Objective) because the Net Heat Flux is usually negative at nighttime.

2.0 OVERVIEW

Net heat flux was proposed as an operational satellite product for the first time by the VIIRS science team. Its four components challenge NPOESS sensors as well as retrieval algorithms. Direct measurements of these parameters are very sparse. Current state-of-the art latent heat flux measurements from buoys achieve an accuracy of only ~20 Wm^{-2}, whereas studies show that current satellite measurements of latent heat flux cannot be obtained to much better than 40 Wm^{-2}. For single matchups (instantaneous), the standard deviation of the latent heat flux between ship and satellite measurements is about 30 Wm^{-2} (Schluessel, 1996).

Satellite remote sensing has been shown to be a viable method for retrieval of net heat flux, although the potential uncertainties are great. Curry et al. (1999) have studied satellite- measured surface net heat flux in detail. They use a high-resolution dataset from the Tropical Ocean Global Atmosphere Coupled Ocean-Atmosphere Response Experiment (TOGA COARE) with a spatial resolution of 50 km and temporal resolution of 3h, and compare the results to fluxes derived from the Special Sensor Microwave/Imager (SSM/I), Advanced Very High Resolution Radiometer (AVHRR), and geostationary weather satellites. Comparisons between satellite-derived and TOGA measured short-wave and long-wave net radiation, latent, and sensible heat flux (Curry et al. (1999)) show a large uncertainty in calculating the surface short-wave net radiation, long-wave net radiation, latent heat flux, and sensible heat flux for three-hourly values (Table 2).

The error calculated from instantaneous comparisons between surface and satellite- derived longwave and shortwave radiation fluxes at the surface are usually so large that only monthly mean satellite data are are reported. The error of the monthly averaged net combined shortwave and longwave flux at the surface is about 10 Wm^{-2} (Darnell *et al*., 1992; Gupta *et al*., 1992; or see http://agni.larc.nasa.gov /model_doc.html).

The satellite retrieval of sensible and latent heat flux depends critically on the estimation of sea surface temperature, sea surface wind, and surface humidity. The VIIRS skin sea surface temperature uncertainty is expected to be about 0.3 K under conditions where the baseline VIIRS SST algorithm can be used *[Y-2386]*. The skin sea surface temperature as measured by a satellite is typically a few tenths of a degree cooler than the bulk temperature needed for net heat flux retrievals (Robinson *et al*., 1984), but can be up to 1 K cooler or warmer in extreme circumstances; this is the so-called “skin effect.” Sea surface wind can also affect sea surface temperature retrieval from space. Sea surface wind speed has generally been calculated from passive microwave sensors such as the Special Sensor Microwave/Imager (SSM/I) (Liu *et al*., 1997) and scatterometers such as QuikSCAT (Graf *et al.*, 1998). The water emissivity can change with sea surface roughness due to sea surface wind (Harris *et al*., 1994). The emissivity of the sea surface changes significantly above viewing zenith angles of about 50 degrees. Turbulent heat transfer is almost a linear function of sea surface wind; errors of ten percent in the retrieval of sea surface wind are the best current research results. A 10 percent (or about 1 ms^{-1}) error in sea surface wind can result in an error of 10 Wm^{-2} in NHF due to the error introduced in the calculation of sensible and latent heat fluxes.

For purposes of deriving turbulent fluxes using the NPOESS system, low- level air temperature and surface humidity may be obtained from the atmospheric profiles of CrIS or CMIS or analysis

from a numerical forecast model. Unfortunately, their accuracy is unlikely to be better than 10 percent in near the future, which is far worse than what is needed to fulfill the NHF requirement. Retrieval accuracy for net heat flux is also affected by atmospheric correction, foam, atmospheric stability, and wind direction. Knowledge of the roughness spectrum of the ocean would be very helpful. One of the NPOESS sensors, CMIS, should be able to derive the sea surface wind speed and direction. Its prototype, "Windsat," is under development.

Table 2. Comparison of the three-hourly surface short-wave net radiation, long-wave net radiation, latent heat flux, and sensible heat flux values between ship measurements and retrievals using satellite data (adopted from Curry et al. 1999, unit: W m^{-2}).

	Net short-wave flux	Net long-wave flux	Latent heat flux	Sensible heat flux
Bias (ship-satellite)	-26	-8	19	-4
Rms error	86	16	45	11
Correlation	0.96	0.35	0.72	0.37

2.1 BACKGROUND

2.1.1 Net longwave radiation

The net longwave radiation over the ocean has been retrieved using different formulas, and the performances of these formulas have been evaluated. Bulk formulas for longwave net radiation over the ocean surface (Anderson 1952) calculate the longwave net radiation at the sea surface from measured sea surface temperature, air temperature, humidity of the boundary layer, and cloud cover. (Since VIIRS Net Heat Flux retrievals will only be conducted under clear conditions, cloud cover should not be a factor in the VIIRS longwave retrievals.) Gilman and Carrett (1994) discussed eight bulk formulas and found that the resulting annual mean difference of the longwave net radiation over the Mediterranean Sea can be up to 20 Wm^{-2}. Zhi and Harshvardhan (1993) calculated the longwave net radiation from a combination of general circulation model cloud radiative forcing fields, cloud radiative forcing at the top of the atmosphere from ERBE (Earth Radiation Budget Experiment), TOVS (TIROS Operational Vertical Sounder) profiles, and sea surface temperatures of ISCCP C1 data. The longwave net radiation (Smith and Woolf 1983) over oceans also can be derived from a passive microwave sensor, such as SSM/I. Gupta (1989) used the International Satellite Cloud Climatology Project (ISCCP) data set to determine the longwave net radiation at the surface.

Our net longwave flux calculation is based on the Gupta *et al.* (1992) algorithm, which is flexible and therefore adaptable in using input data from a wide variety of sources. This algorithm is based on parameterized equations developed expressly for computing surface longwave radiation in terms of meteorological parameters which should be available from satellite data/or other operational sources, as described in Sections 3.2 and 3.3.2.1. The main inputs of the Gupta *et al.* (1992) algorithm are surface temperature and emissivity, atmospheric profiles of temperature and humidity, fractional cloud amounts, and cloud heights. The algorithm equations are based secondarily on the physics of radiative transfer, as they were developed from a large database of surface fluxes computed with an accurate, narrow-band radiative transfer model.

Some of these parameters will be derived from other instruments on the NPOESS platform, but timing constraints on the data processing may prevent use of data obtained simultaneously on the same NPOESS platform.

2.1.2 Net Shortwave Radiation

To derive net shortwave radiation from satellite data, a statistical relationship between the reflected radiation field at the top of the atmosphere (TOA) and at the surface is often applied. This method is utilized in the VIIRS NHF algorithm. The relationship between TOA and surface shortwave radiation is affected by the solar zenith angle, gaseous and aerosol absorption and scattering, and surface reflectivity. Because atmospheric constituents absorb and scatter, but do not emit radiation at solar wavelengths, there is a coupling between the radiation fields at the top of the atmosphere and at the surface (Schmetz 1989). The character of the coupling depends on the absorption within the atmosphere. In contrast to the strong variability of the radiation budget at the top of the atmosphere and at the surface, atmospheric absorption remains relatively stable. However, small changes in the magnitude of the atmospheric absorption are correlated with changes in the reflected shortwave flux at the top of the atmosphere (Li *et al*. 1993). This effect generates a portion of the forward modeling error in the VIIRS SW algorithm error budget.

Darnell and Staylor (1988) modified this approach for calculating the surface shortwave radiation. The basic idea of this approach is that the surface solar radiation is approximately a product of sun irradiance at the top of the atmosphere and the "effective transmission." The effective transmission is a resultant optical depth arising from all absorption and scattering processes acting on the vertical radiation. Individual, well-developed vertical optical depth models are available to represent most of these atmospheric scattering and absorption processes. The optical depths of these separate components are generally either small or spectrally nonoverlapping. The effective transmission is a function of water vapor, ozone, carbon dioxide, oxygen, molecular scattering, surface albedo effects, and aerosol effects. The Li et al (1993) and Darnell and Staylor (1988) algorithms were developed based on radiation flux at the top of the atmosphere, where the radiation flux is either from ERBE measurements or calculated from narrow band radiances such as those obtained from instruments similar to VIIRS.

2.1.3 Sensible and Latent Heat Fluxes

There are four standard techniques for measuring sensible and latent heat fluxes (Chou 1993): (a) eddy correlation; (b) inertial subrange dissipation; (c) mean profiles; and (d) bulk aerodynamic methods (e.g., Paulson *et al*., 1972; Kondo 1975; Garratt 1977; Large and Pond 1981; Blanc 1987). Only the eddy correlation method is a direct measure of the fluxes. It requires a time series of vertical wind, horizontal wind, and temperature and humidity fluctuations. The measurement of vertical wind requires a rigid, slender supporting structure to avoid contamination due to motion and flow distortion of the supporting structure. The inertial subrange dissipation method estimates fluxes from the budget equations and the dissipation of turbulent kinetic energy, temperature, and humidity variances. The dissipation variables are determined from the spectra of wind, temperature, and humidity in the inertial subrange. The subrange occurs at frequencies higher than those of dominant ocean waves and ship or buoy motions. Thus the dissipation method is relatively insensitive to platform motions. After verification, this method can be applied to a larger range of experimental sites and conditions

than the eddy correlation method. The flux-profile relationships describe relations between the surface fluxes and the mean profiles (gradients) of wind, temperature, and humidity in the atmospheric surface layer. Flux measurements by the profile and dissipation methods are based on these relationships. For the VIIRS Net Heat Flux EDR, the bulk formula method is used.

The bulk formula is often used to calculate sensible and latent heat fluxes (Chou *et al.* 1995) because of its extensive use in numerical models and its applicability to a large scale of climatological data sets from ships or buoys or from satellite measurements (Crewell *et al*. 1991). The bulk formula method used for the derivation of the sensible and latent components of the VIIRS NHF is described in Section 3.3.2.3 of this document. The greatest difficulty in deriving bulk sensible and latent fluxes from space is that the measured radiance is not sensitive to air temperature and surface humidity. The bulk coefficient (Budyko 1974) is also an empirical coefficient, and is not well known. The development of a reliable bulk scheme, based on direct eddy-correlation measurements, is essential (Isemer and Hasse 1985).

2.2 VIIRS INSTRUMENT REQUIREMENTS AND CALIBRATION

The VIIRS Net Heat Flux EDR is calculated from calibrated VIIRS radiances, other VIIRS EDRs, and data from non-VIIRS NPOESS instruments. To approximate the solar radiative flux at the surface, VIIRS radiances (which are dependent on scatter by molecules and aerosols and absorption by water vapor and ozone) are required. Net longwave fluxes at the ocean surface can be obtained by combining data from VIIRS surface temperature EDRs with atmospheric profiles from other sources. The sensible and latent components of NHF are derived from non-VIIRS atmospheric profiles in combination with the VIIRS SST and IST EDRs, so they do not drive VIIRS sensor models.

Several sensor noise models have been constructed, with model 0 representing a perfect sensor, and sensor performance progressively degrading as model number increases. It can be seen from Figure 6 that sensor model 3 or better satisfies the EDR requirement for precision, where results are derived based on the baseline set of wavelengths given in Table 3. This sensor model was used for flowdown of the sensor design. The final VIIRS model is better than the sensor model 3.

The required VIIRS wavelengths and bandwidths are provided in Table 3. The direct derivation of the downwelling shortwave radiation flux may relax the requirement on other EDRs such as aerosols and ozone as well as the humidity profile. The shortwave radiation flux at the top of the atmosphere, as calculated from the baseline sensor design, can satisfy the EDR uncertainty and precision requirements for shortwave net flux at the surface. However, the anticipated uncertainties of other VIIRS EDRs and auxiliary data used in the VIIRS NHF algorithm make meeting threshold requirements for accuracy and precision impossible (see Table 1 and the error analysis in Section 3.3.4.1).

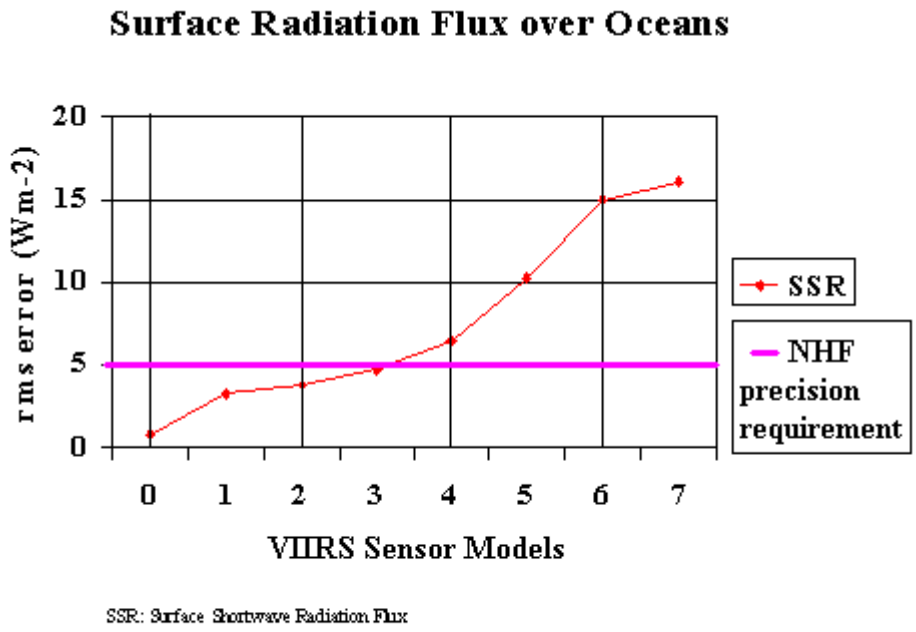

Figure 6. Retrieval errors for different VIIRS sensor models. Sensor model 0 represents a perfect sensor.

Table 3. Wavelength and bandwidth of VIIRS bands used for NHF EDR. The minimum and maximum wavelength for each band are given in µm.

M1	M2	M3	M4	M5	M6	M7	M9	M10	M11	M14	M15	M16
0.402-0.422	0.435-0.455	0.478-0.498	0.545-0.565	0.662-0.682	0.739-0.754	0.845-0.884	1.371-1.386	1.580-1.640	2.225-2.275	8.40-8.70	10.26-11.26	11.54-12.49

Absolute calibration is required for calculating the shortwave radiation fluxes, and calibration errors must be included in the error budget. For shortwave radiation, a calibration error of less than 0.5 percent is required, but this is unrealistic for initial calibration considering cost and existing technology. However, this level of calibration accuracy should be achievable by using more precise radiation budget measurements from other instruments (such as CERES) or in situ observations to adjust VIIRS-derived radiation fluxes at the top of the atmosphere and at the surface. If surface-based observations are used, calibration depends on a radiative transfer code such as MODTRAN (Berk *et al.*) and knowledge of atmospheric conditions.

The algorithm described in this document is capable of producing the NHF EDR with only VIIRS data and required auxiliary data that may derive from any other source. The source of

auxiliary data may be other NPOESS instruments or meteorological analyses from NCEP. If data from multiple NPOESS instruments can be integrated during EDR processing, the use of microwave radiance or brightness temperatures from CMIS at 6.8, 10.7, 19.35, 22.235, 37, 85.5 GHz and other channels at 60 GHz and 183 GHz would be beneficial. The brightness temperature at 6.8 GHz is sensitive to sea surface temperature. The brightness temperatures at 10.7 and 19.35 GHz should be optimal for determining sea surface wind. Channels 19.35, 22.235, 37, 85.5 GHz have also been used in many applications.

3.0 ALGORITHM DESCRIPTION

The Net Heat Flux EDR is a measurement of energy balance over the oceans. This energy balance has been described by radiative transfer theory and turbulence theory. An important constraint for the surface flux is the conservation of total energy. The equation for the heat budget of an interfacial layer is fairly complex because many energy transfers and transformations from one form of energy to another have to be taken into account. These processes take place continuously both at and near the ocean's surface. Most of the transformations start with the absorption of solar radiation and end with the loss of infrared radiation to space. The complete energy cycle is described as follows:

The absorbed solar radiation leads to an increase in the heat content of ocean mixed layer. This thermal energy may, in turn, lead to an upward transfer of sensible, latent, and longwave radiation energy into the atmosphere and a downward transfer of heat into the ocean below the mixed layer. Therefore, turbulent theory is applied to determine the bulk coefficients used in the calculation of sensible and latent heat fluxes. A detailed discussion of the theory of sensible and latent heat transfer within the atmospheric boundary layer can be found in Brutsaert (1982). Refer to Section 3.3.2.4 for a more detailed description of the derivation and use of the bulk coefficients for calculating sensible and latent heat fluxes for the VIIRS NHF EDR.

The physics of the interaction of shortwave and longwave radiation with the atmosphere can be described by radiative transfer theory. Much can be found about radiative transfer theory in the literature, including polarized and nonpolarized problems. There are one-dimensional, two-dimensional, and three-dimensional radiative transport theories. For one-dimensional radiative transfer, two-stream, successive orders of scattering and matrix operator methods are often applied. Radiative transfer models are available at many spectral resolutions, including very high resolution line-by-line models, the Moderate Resolution Atmospheric Radiance and Transmittance Model (MODTRAN), the Low Resolution Atmospheric Radiance and Transmittance Model (LOWTRAN), and narrow-band models.

For shortwave radiation, the solar incident radiation flux at the top of the atmosphere is a sum of the shortwave net radiation at the surface, absorbed radiation by the atmosphere, and the reflected radiation flux at the top of the atmosphere. The surface albedo, or fraction of incident shortwave radiation at the surface that is reflected, is also a significant control on net shortwave radiation absorbed at the surface. For clear sky cases, the reflected shortwave radiation flux at the top of the atmosphere has a strong linear correlation with the part absorbed by the atmosphere. Thus, it is reasonable to assume a linear relationship between the satellite-measured radiance and the shortwave net radiation over the ocean surface. A second simulation of the satellite signal in the solar spectrum (6S) has been applied to simulate the shortwave radiation flux at surface and satellite-borne VIIRS radiances. These initial simulations assumed a simplified sensor response function for each VIIRS channel, but once information about the actual VIIRS band response functions becomes available it will be used in further error analysis and possible algorithm or look-up table adjustment. The 6S code (Vermote *et al.* 1997) enables simulation of plane-parallel conditions, taking into account non-lambertian surface boundary conditions. New gases (CH4, N2O, CO) have been integrated into computation of the gaseous transmission.

The selection of 6S or MODTRAN has no influence on the logic of the algorithm. However, it is preferable to base the shortwave retrievals on MODTRAN, since it is complex but versatile, with many successful applications. MODTRAN also models the absorption of radiation by gases in the atmosphere more accurately. MODTRAN 3.7 has 1/cm spectral resolution in the visible and infrared regions and 5/cm in the ultraviolet area. Two-stream and DISORT (Discrete Ordinate Radiative Transfer) are available in the code. MODTRAN is faster than line-by-line models, but it is not fast enough to be executed operationally in the NHF calculation, so it will be used to create look- up tables for use in the shortwave and longwave flux calculations. More information about MODTRAN is available on the World Wide Web at http://www2.bc.edu/~sullivab/soft/modtran4.html

Derivation of the longwave net radiation is difficult because the atmosphere and surface emit longwave radiation separately. There is no clear correlation between the longwave radiation at the surface and at the top of the atmosphere. MODTRAN version 3.7 code has been used to simulate the longwave net radiation over the oceans and the VIIRS radiance. The results of these MODTRAN simulations are combined with surface temperature and atmospheric profile information to obtain net longwave flux at the surface.

CMIS or NCEP wind speeds are used in the derivation of ocean surface albedo for the shortwave radiation flux calculation. The anticipated error in these wind speed data is ten percent, or about one meter per second, at wind speeds of less than 25 m s^{-1}. The effects of surface wind speed error are analyzed in the error analysis and algorithm sensitivity studies of this document (Sections 3.3.4.1 and 3.4.3). It is also possible to use CMIS data in the derivation of longwave and latent heat fluxes, but this approach is not the one described in the VIIRS Net Heat Flux Detailed Design *[Y-3230]*. To simulate CMIS microwave brightness temperatures, polarization must be considered. The matrix operator method is one of the commonly used methods, which accounts for scattering and polarization. For a homogeneous layer, the matrix operator method solves the radiative transfer equation in analytical matrices. The solution of the radiative transfer equation for the vertically inhomogeneous atmosphere is obtained recursively from the analytical solutions for a set of homogeneous layers, where the vertically inhomogeneous atmosphere is subdivided into a set of homogeneous layers (Liu and Ruprecht, 1996).

3.1 PROCESSING OUTLINE

The four components of Net Heat Flux- longwave radiation, shortwave radiation, sensible heat flux, and latent heat flux- are calculated separately. The longwave net radiation flux, L_{net}, will be calculated from atmospheric profiles from CrIS EDRs or NCEP and the VIIRS sea surface temperature EDR. Figures 7-10 indicate the flow of simulated VIIRS and auxiliary data through the algorithms for calculating each component of the Net Heat Flux EDR, as well as the anticipated data flows in the operational VIIRS system. In Figure 7, a regression technique is applied to calculate L_{net} from the sea surface temperature and temperature and humidity profiles of the atmosphere. Shortwave net radiation, S_{net}, (see Figure 8) over the oceans can be calculated directly from the VIIRS radiances. Comparison of retrieved S_{net} with surface observations or the reflected shortwave radiation flux at the top of the atmosphere through an empirical equation is recommended. Sensible, H, and latent, E, heat fluxes are calculated (see Figures 9 and 10) from VIIRS sea or ice surface temperature, and air temperature and specific

humidity interpolated from CrIS or NCEP temperature and humidity profiles. Bulk formulas are applied, the coefficients of which are dependent on the sea surface wind and temperature difference between air and ocean.

Since S_{net} is dependent only on VIIRS radiances, an independent value can be calculated for each VIIRS pixel and then aggregated into 20 km cells. A threshold fraction of pixels within a grid cells that may contaminated by clouds or other obstructions without causing significant errors will be determined, and grid cells containing more than that fraction of non-clear pixels will be flagged and filled with fill values. The other components of NHF depend on CrIS profiles along with VIIRS surface temperature information, so input information from both sources is aggregated to the 20 km cells before the flux calculations are performed. Ice cover fraction will be determined for each clear ocean pixel using the VIIRS Ice Concentration Application Related Requirement. The VIIRS Ice Concentration values will have an associated 10% uncertainty *[Y-2466]*; the impact of this uncertainty is evaluated in our error budget (Section 3.3.4.1). If a grid cell is mixed water and ice, longwave and turbulent fluxes will be calculated separately for water and ice, then combined in a weighted average according to the fraction of valid pixels within the cell that are ice.

3.2 ALGORITHM INPUT

3.2.1 VIIRS Data

Information from the VIIRS Cloud Mask IP, VIIRS radiances from the reflective bands in Table 3, and the VIIRS Surface Albedo EDR, are used to calculate the shortwave net radiation flux over the ocean surface. VIIRS SST and IST EDRs are used in the calculation of longwave, sensible, and latent heat fluxes.

3.2.2 Non-VIIRS Data

The Net Heat Flux EDR requires additional, non-VIIRS information, including temperature and humidity profiles from CrIS EDRs or NCEP analyses, and sea surface winds derived from CMIS or NCEP. The coefficients needed to convert VIIRS radiances to values of net shortwave radiation at the surface are held in a look- up table, with parameters shown in Table 4 below.

Table 4. Look-up Table Parameters for Deriving Short-Wave Radiation at the Surface from VIIRS radiances.

Parameter	Definition
Wavelength	All VIIRS bands having wavelengths less than 3700 nm.
Surface pressure	Generated at a standard pressure of 1013.25 hPa.
Sea Surface Wind Speed	10 m/s at 10 meters above the sea surface.
Solar zenith angle	16 Gauss discrete angles, which covers 0 to about 85 degrees.
Viewing zenith angle	16 Gauss discrete angles, which covers 0 to 85 degrees.
Relative azimuth angle (solar/viewing)	Every 10 degrees beginning from 0.
Aerosol types	Maritime, coastal, continental, and urban aerosols have 10 optical thicknesses at 555 nm between 0.05 and 3.
Ozone Amount	Ozone amount at 100, 200, 300, 400, and 500 Dobson Unit.
Atmospheric profiles	At least six standard atmospheric profiles.
Ice Surface Albedo	At values of 0.6, 0.8, and 1.

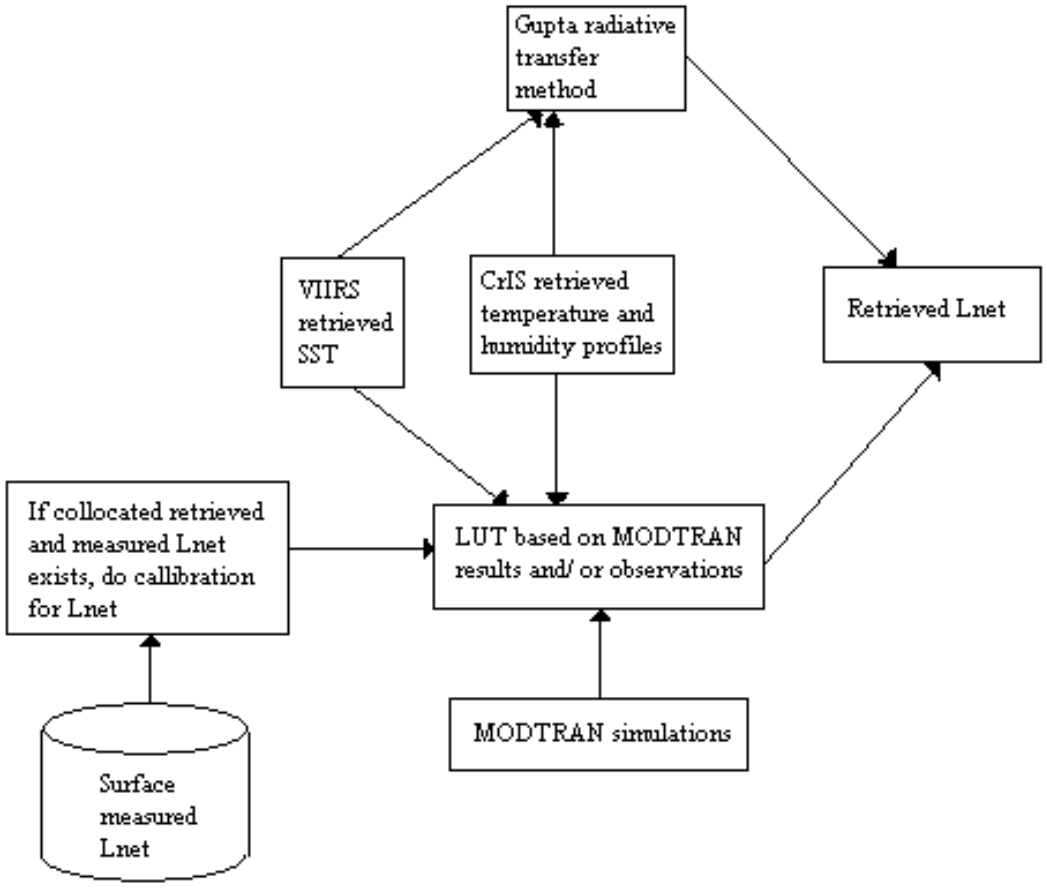

Figure 7. EDR flowdown process diagram for L_{net}. The Gupta radiative transfer method is currently implemented.

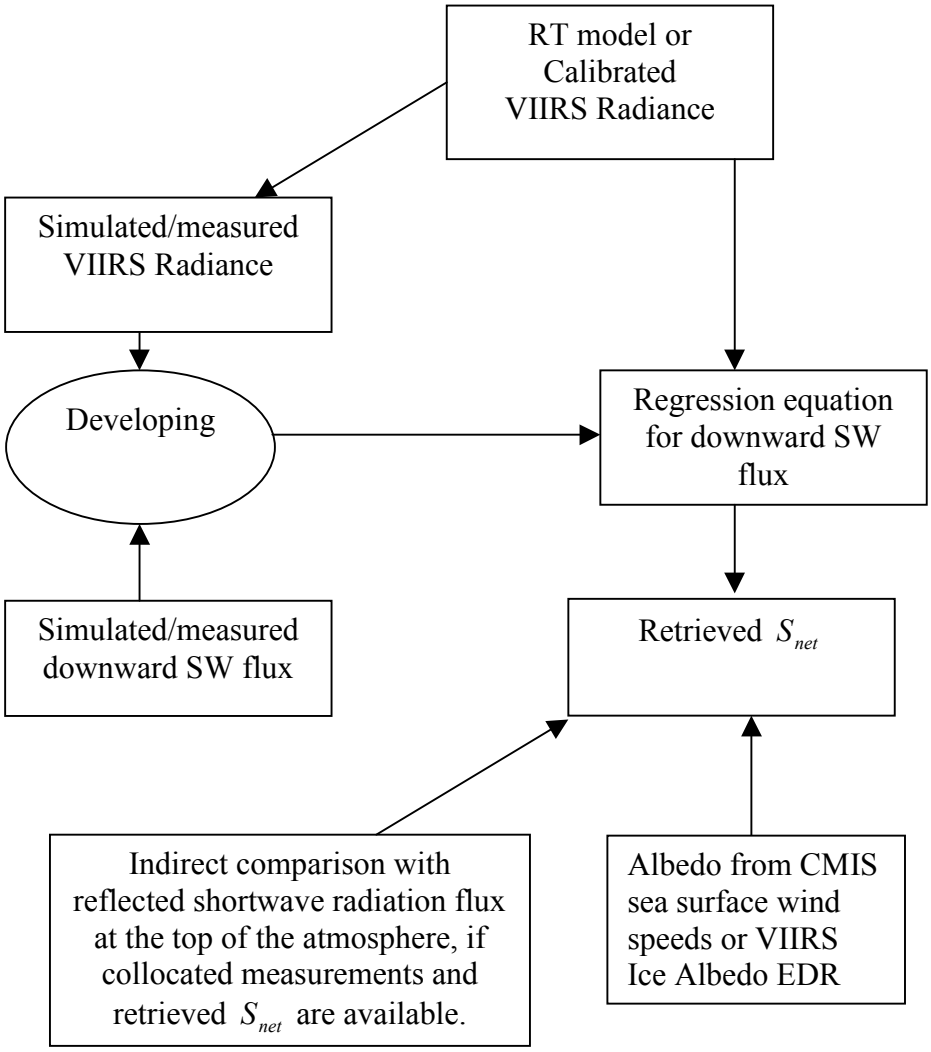

Figure 8. EDR flowdown process diagram for S_{net} .

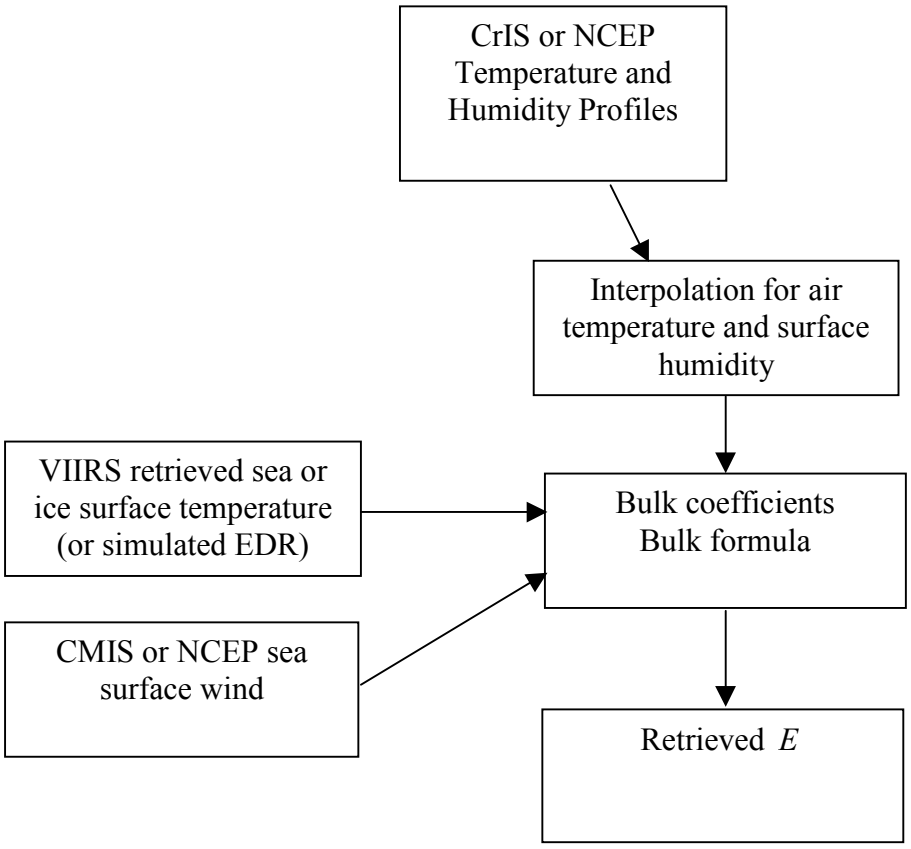

Figure 9. EDR flowdown process for latent heat flux.

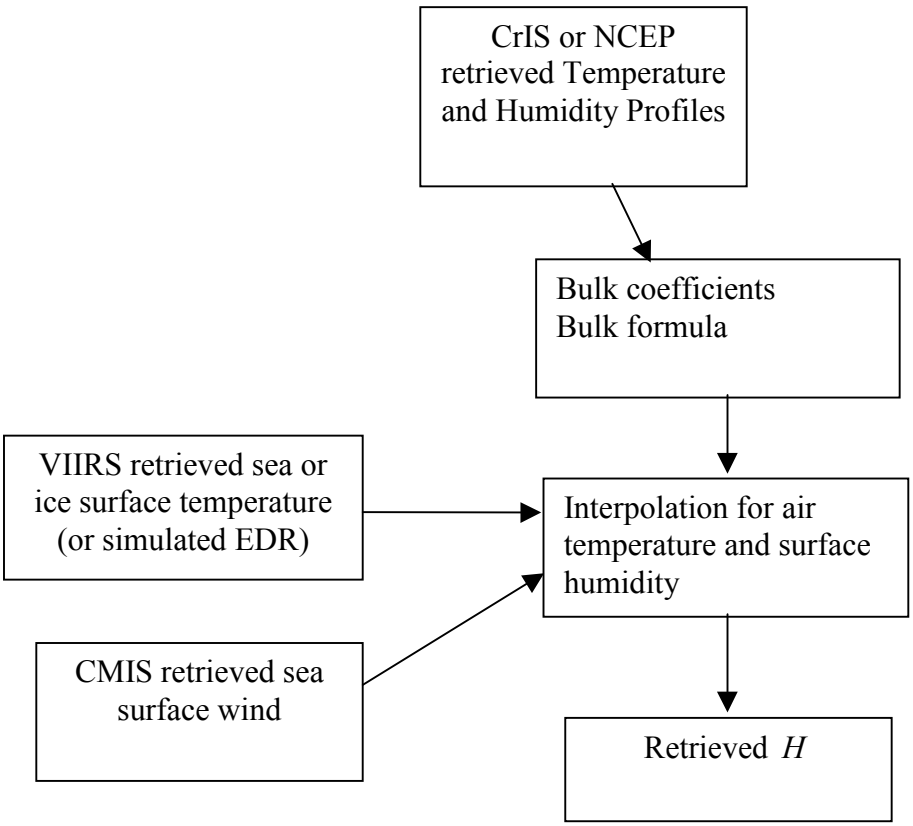

Figure 10. EDR flowdown process for sensible heat flux.

3.3 THEORETICAL DESCRIPTION OF NET HEAT FLUX RETRIEVALS

3.3.1 Physics of the Problem

Net Heat Flux is governed by radiative and turbulent processes. There is no direct relation between satellite-measured radiance and the downward longwave and shortwave radiation (Fung *et al.,* 1984). Because VIIRS and other NPOESS sensors used for the Net Heat Flux EDR measure only the directional narrow–band radiance at the top of the atmosphere, the physics of retrieval of the surface radiation is composed of three parts: a) calculating downward narrow-band radiance at the surface by atmospheric correction for shortwave radiation or by statistical relation for longwave radiation; b) converting narrow-band radiance to broad-band radiance (0.2 – 4 μm for shortwave, 4 – 400 μm for longwave); and c) converting the directional broadband radiance to the angular integrated irradiance. The modeling or observations used to generate the regression coefficients for the shortwave calculation must take each of these steps into account. The longwave net radiation over the ocean surface depends on the vertical structure of the temperature and humidity profile and sea surface temperature. VIIRS IR radiances are

insufficient to take into account the vertical structure. At present, L_{net} is either calculated from the CrIS or NCEP temperature and humidity profiles. This retrieval is based on radiative transfer model calculations of flux given the atmospheric state.

The latent and heat fluxes are forms of turbulent, as opposed to radiant, energy. Both fluxes affect satellite-measured radiances or brightness temperatures because they relate to the atmospheric state. The main weaknesses in the methods used to determine latent and sensible heat fluxes are validity of the bulk formula, the bulk coefficient, the air temperature near the surface, and the surface humidity.

3.3.2 Mathematical Description of the Algorithm

The retrieval algorithms for the radiative and turbulent components of NHF are independent. Mathematical methods which may be used to derive each of the net heat flux components are described below.

3.3.2.1 Longwave Net Radiation Flux Calculated From Atmospheric Profiles and VIIRS SST/ IST

The method described here is the one implemented in the VIIRS Net Heat Flux Detailed Design *[Y-3230],* that will be converted into operational code.

L_{net} can be calculated from a radiative transfer model if the atmospheric state is known. However, such computations are too expensive for operational satellites. According to an empirical formula developed by Gupta *et al*. (1992), L_{net} over the ocean surface can be expressed as:

$$L_{net} = \varepsilon_{IR}(F_d - \sigma T_s^4) \tag{1}$$

where σ is the Stefan-Boltzman constant, T_s is sea surface temperature. ε_{IR} is the longwave emissivity of the sea surface and its value is commonly assumed to be 0.98 (e.g. Gilman and Carret, 1994). The downward longwave radiation flux for a clear sky case is represented as:

$$F_d = (A_0 + A_1 V + A_2 V^2 + A_3 V^3) T_e^{3.7} \tag{2}$$

(Gupta *et al*. 1992), where $V = \ln W$, W is the total perceptible water obtained from the CrIS or NCEP profile, and T_e is an effective emitting temperature of the lower atmosphere. T_e is calculated as:

$$T_e = k_s T_s + k_1 T_1 + k_2 T_2 \tag{3}$$

The coefficients in (2) and (3) are as follows:

$$A_0 = 1.791\times10^{-7}, \quad A_1 = 2.093\times10^{-8}, \quad A_2 = -2.748\times10^{-9}, \quad A_3 = 1.184\times10^{-9}$$
$$k_s = 0.60, \quad k_1 = 0.35, \quad k_2 = 0.05$$

where T_1 and T_2 are the mean temperatures of the first and second atmospheric layers next to the surface. These layers cover the surface-800 mb, and 800-680 mb regions obtained from CrIS or NCEP temperature profiles.

In the future, a look-up table based on MODTRAN or another radiative transfer model could be implemented to derive net longwave fluxes from surface temperature and atmospheric profile data, as shown in Figure 7.

3.3.2.2 Longwave Net Radiation Flux Calculated From CMIS Brightness Temperature

There is an alternative method for deriving net longwave radiation fluxes, which is not currently implemented in the VIIRS prototype code. It requires the use of a neural network, which is described in Version 4 of this document. A neural network approach is also a possible method of deriving latent heat fluxes from CMIS brightness temperatures. The method for obtaining latent heat fluxes using a neural network is also described in Version 4 of the VIIRS Net Heat Flux ATBD.

3.3.2.3 Shortwave Radiation Flux

The downward shortwave radiation flux at the surface can be calculated if the atmospheric state (e.g., surface reflectivity, aerosols, and humidity profiles) and the downward shortwave radiation at the top of the atmosphere are known. The shortwave radiation flux can be calculated directly from VIIRS radiances for the proposed ten shortwave channels because the VIIRS measurements contain that atmospheric information, and the shortwave radiation flux is not sensitive to the vertical distribution of the temperature and moisture profiles. A regression algorithm is applied to calculate the downward shortwave radiation flux at the surface (SW) for given sun incidence and satellite viewing angles:

$$SW = a_0 + \sum_{k=1}^{10} a_k R_k \tag{4}$$

In Equation (4), k runs through the ten reflective bands used in the VIIRS shortwave retrieval. The regression coefficients, a_k, are determined by minimizing the root mean square error between VIIRS- retrieved radiances (R_k) and fluxes obtained from a radiative transfer model for the corresponding sun incidence and satellite viewing angle. (Before actual VIIRS data become available, simulated VIIRS radiances will be produced by combining a VIIRS sensor model with the radiative transfer model.) A look-up table of coefficients for use in Equation (4) will be generated by simulating the radiative transfer over a range of solar and sensor geometries, aerosol types, atmospheric profiles, and ozone amounts. Once SW is calculated, net shortwave flux can be derived:

$$Net\ SW = (1-\alpha)SW \tag{5}$$

and the surface albedo of the ocean is expressed, following Hansen et. al. (1983):

$$\alpha = 0.021 + 0.0421\,x^2 + 0.128\,x^3 - 0.04\,x^4 - \left[3.12/(5.68 + WS) + (0.074x)/(1 + 3\,WS)\right] x^5 \quad (6)$$

where $x = 1 - \mu_0$, μ_0 is the cosine of the sun zenith angle and WS is the surface wind speed in units of m/s.

3.3.2.4 Sensible and Latent Heat Fluxes

Based on the eddy correlation approach, the sensible heat flux can be expressed as:

$$H = \rho c_p \left\langle w'\theta' \right\rangle \quad (7)$$

or

$$H = \rho c_p \left\langle w'T' \right\rangle \quad (8)$$

where ρ is the air density, c_p the specific heat of air at constant pressure, and w', T' and θ' the deviations from the time averaged vertical velocity, temperature, and potential temperature, respectively. Equations (7) and (8) are approximately equivalent, since near the surface $T' \approx \theta'$. Thus, in principle, the vertical fluxes can be evaluated from the direct measurements of w' and T'. However, it is very difficult to obtain w', which prevents the use of this method. The sensible flux of heat can be written on the basis of the Prandtl assumption:

$$H = \rho c_p \left\langle w'\theta' \right\rangle = -K_H \rho c_p \left\langle \frac{\partial \theta}{\partial z} \right\rangle \quad (9)$$

where K_H is the eddy diffusion coefficient for heat. This equation implies that the vertical flux of heat is determined by the mean vertical potential temperature gradient. It also corresponds to the intuitive idea that heat flowing from warm to cold regions is proportional to the gradient of the mean potential temperatures. Over the oceans, (9) can be approximately expressed by:

$$H = \rho c_p C_H (V - V_s)(T_s - T_A) \quad (10)$$

where C_H is the bulk coefficient, V is the horizontal wind speed at a height of 10m, T_s is the sea surface temperature, and T_A is the air temperature. V_s is the horizontal wind speed at the surface. c_p is the isobaric specific heat.

According to Fick's law, the net vertical flux of water vapor across the earth's surface is proportional to the vertical gradient of specific humidity (similar to sensible heat). The proportionality coefficient for the water vapor flux ,α_w ,is the molecular diffusivity for water vapor:

$$E = -\rho \alpha_w \left\langle \frac{\partial q}{\partial z} \right\rangle \quad (11)$$

This expression is only valid in the laminar viscous sublayer, where molecular exchange is the prevalent transfer mechanism. The lower region of the surface boundary layer is almost always turbulent so that in this layer the water vapor is transferred away from the molecular sublayer by turbulence. The vertical flux is then given by:

$$E = \rho c_p \left\langle w' q' \right\rangle \tag{12}$$

The transport in this mixed layer depends on ocean surface roughness, wind shear, and thermal stratification. Therefore, the rate of transfer of water vapor (evaporation) depends on all these factors as well as on the gradient of specific humidity. Then, a gradient-flux relation can be accepted and expressed in a bulk formula:

$$E = \rho L C_w (V - V_s)(q_s - q_A) \tag{13}$$

where L is the latent heat of vaporization. Its value is approximately $L = 2.456 \times 10^6 \, Jkg^{-1}$. The mean q_s is generally assumed to be the saturation value at T_s. Air density can be calculated from near- surface pressure and temperature values using the ideal gas law, or approximated as $\rho = 1.15 \, kgm^{-3}$.

For a simple case (i.e., neutral condition), the bulk coefficients are:

$c_p = 1005 Jkg^{-1}K^{-1}$ (Gilman and Carrett, 1994),

$C_w = 1.14 \times 10^{-3}$, $C_h = C_w / 1.2$

These values can be used as constants in a simplified version of the bulk transfer equations. However, for more accurate calculations, it should be taken into account that bulk coefficients for neutral conditions and unstable cases are different. Cold air blowing over warm water is heated from below and tends to convect. The air column becomes unstable, and the transfer of heat no longer depends solely on the turbulence generated by wind shear; rather, it is augmented with the turbulence generated by temperature instability.

Under unstable conditions, the bulk coefficient for momentum is:

$$\tau = \rho C_D (V - V_s)^2 \tag{14}$$

where τ is the wind stress. Based on the surface-layer similarity theory, Liu *et al.* (1979) developed a bulk scheme with stability-dependent transfer coefficients. According to the theory, the mean diabatic profiles of V, θ and q, with a stability parameter $\xi = Z / L$ (where Z represents height above the surface and L is the Monin-Obukhov length) may be expressed as (e.g., Paulson, 1972):

$$(V - V_s) / u_* = \left[\ln(Z / Z_M) - \varphi_M(\xi) \right] / k_M \tag{15}$$

$$(\theta - \theta_s) / \theta_* = \left[\ln(Z / Z_H) - \varphi_H(\xi) \right] / k_H \tag{16}$$

$$(q - q_s)/q_* = [\ln(Z/Z_E) - \varphi_E(\xi)]/k_E \quad (17)$$

where the subscripts M, H, E indicate the quantities related to momentum, sensible heat and moisture, respectively. k_M, k_H, and k_E are various von Kármán constants, and are assigned 0.4, 0.45, and 0.45 by Liu *et al*. (1979), respectively. Z_M, Z_H, and Z_E are the various roughness lengths. The profile scaling parameters are given by:

$$u_* = (\tau/\rho)^{1/2} \quad (18)$$

$$\theta_* = -H/(\rho c_p u_*) \quad (19)$$

$$q_* = -E/(\rho L_v u_*) \quad (20)$$

The three stability functions, ϕ_M, ϕ_H, and ϕ_E, are related to the three dimensionless gradients, φ_M, φ_H, and φ_E, by the following expression:

$$\phi(\xi) = \quad (1-\varphi)d\ln\xi \quad (21)$$

For unstable stratification, ϕ can be expressed as:

$$\phi_M = 2\ln[(1+(1-16\xi)^{1/4}/2] + \ln[(1+(1-16\xi)^{1/2}/2] - 2\tan^{-1}(1-16\xi)^{1/4} + \pi/2 \quad (22)$$

$$\phi_H = 2\ln[(1+(1-16\xi)^{1/4}/2] \quad (23)$$

$$\phi_E = 2\ln[(1+(1-16\xi)^{1/4}/2] \quad (24)$$

For the stable stratification, they are generally given as:

$$\phi_M = \phi_H = \phi_E = 1 + a\xi \quad (25)$$

where a is a constant approximately equal to 5 (Sorbjan 1989, p.76). Including the effect of moisture on buoyancy, ξ can be defined as:

$$\xi = Zgk_M\theta_{v*}/(\theta_v u_*^2) \quad (26)$$

where g is the gravitational acceleration, θ_v is the virtual potential temperature, and:

$$\theta_{v*} = \theta_*(1+0.61q) + 0.61\theta q \quad (27)$$

The lower boundary parameters (Z_M, Z_H, and Z_E) are functions of τ and fluid properties. In order to have a gradual transition from smooth to rough flow, Z_M is assumed to be (Kondo, 1975):

$$Z_M = 0.0144 u_*^2 / g + 0.11 \nu / u_* \quad (28)$$

where ν is the kinematic viscosity of air. The values of Z_H and Z_E determined from the viscous interfacial-sublayer model of Liu *et al*. (1979) are given as functions of roughness Reynolds number $R_r = Z_M u_* / \nu$ as below:

$$Z_H u_* / \nu = a_1 (Z_M u_* / \nu)^{b_1} \quad (29)$$

$$Z_E u_* / \nu = a_2 (Z_M u_* / \nu)^{b_2} \quad (30)$$

where the values of a_1, a_2, b_1, b_2 for different ranges of R_r are given in Table 6 (adopted from Table 1 of Liu *et al*. [1979]).

Table 5. The lower boundary values of the logarithmic profiles.

R_r	a_1	b_1	a_2	b_2
0 - 0.11	0.177	0	0.292	0
0.11 - 0.825	1.376	0.929	1.808	0.826
0.825 - 3.0	1.026	-0.599	1.393	-0.528
3.0 - 10.0	1.625	-1.018	1.956	-0.870
10.0 - 30.0	4.661	-1.475	4.994	-1.297
30.0 - 100.0	34.904	-2.067	30.790	-1.845

With a suitable choice of von Kármán constants (k_M, k_H, and k_E) and unstable, dimensionless gradients (ϕ_M, ϕ_H, and ϕ_E), the three unknowns (τ, H, and E) can be determined by solving the three simultaneous equations 15-17 iteratively. The application of this model is similar to the use of a bulk aerodynamic scheme with variable transfer coefficients, which depend on atmospheric stability and surface roughness. The bulk coefficients can be expressed as:

$$C_D = k_M^2 / [\ln(Z / Z_M) - \phi_M(\xi)]^2 \quad (31)$$

$$C_H = C_D^{1/2} k_H^2 / [\ln(Z / Z_H) - \phi_H(\xi)]^2 \quad (32)$$

$$C_E = C_D^{1/2} k_E^2 / [\ln(Z / Z_E) - \phi_E(\xi)]^2 \quad (33)$$

The bulk parameterization is used for calculating sensible and latent heat fluxes from VIIRS and auxiliary data. This parameterization of sensible and latent heat exchange is frequently used in atmospheric modeling and in interpreting other observational data. Knowledge of the surface roughness is important in applying the bulk parameterization, but since the ocean surface roughness is generally less variable than that of land surfaces and can be related to the surface wind speed, the bulk parameterization should be relatively straightforward to apply given sufficiently accurate surface and near-surface temperature, humidity, and wind speed data. Sea or ice surface temperature will be obtained from the VIIRS SST or IST EDR. If both water and ice surfaces are assumed evaporate until the atmosphere immediately above them is saturated, the surface specific humidity can be calculated by assuming a relative humidity of 100%. Atmospheric profiles of temperature and relative humidity obtained from CrIS or NCEP can be interpolated to obtain values for near-surface temperature and humidity. Sea surface wind speeds

will be obtained from CMIS or NCEP. Once actual data are available, they should be evaluated to ensure that they are consistent enough with each other and with surface-based observations to yield accurate turbulent flux values.

3.3.3 Archived Algorithm Output

Net Heat Flux is a required VIIRS EDR. All components of NHF (surface longwave net radiation, surface shortwave radiation, latent and sensible heat flux) and the outgoing longwave radiation flux as well as the outgoing shortwave radiation flux at the top of the atmosphere will also be produced because they are of great utility for different applications.

3.3.4 Variance and Uncertainty Estimates

The dynamic range of the four components of Net Heat Flux is very large. Over oceans longwave net radiation can change from –50 Wm^{-2} to 150 Wm^{-2}. Shortwave net radiation flux varies from 0 Wm^{-2} to 1200 Wm^{-2}, sensible heat flux changes from –20 Wm^{-2} to 100 Wm^{-2}, and latent heat flux varies from –50 Wm^{-2} to 250 Wm^{-2}. The uncertainty estimate is 5-10 Wm^{-2} for longwave net radiation, 5-10 Wm^{-2} for the shortwave net radiation flux, 10-15 Wm^{-2} for sensible heat flux, and 20-25 Wm^{-2} for latent heat flux, based on simulation results.

3.3.4.1 Error budget

The error due to the VIIRS radiances on net heat flux EDR is small, and the error due to uncertainties in VIIRS-derived EDRs is modest except for those introduced by a lack of precision in the surface specific humidity (derived from sea or ice surface temperature), and by a lack of accuracy in the surface albedo over ice.

As an example of determining a portion of the error budget for longwave radiation, the error for the upward longwave radiation flux, $LWup$, can be derived, where $LWup$ can be expressed as:

$$LWup = \varepsilon \, \sigma \, T_s^4 \tag{34}$$

The error for $LWup$ by sea surface temperature is:

$$\begin{aligned} \Delta LWup &= 4\varepsilon \, \sigma \, T_s^3 \, \Delta T_s \\ &= LWup \, 4 \, \frac{\Delta T_s}{T_s} \end{aligned} \tag{35}$$

For $T_s = 300K$, $\Delta T_s = 0.2K$, $\varepsilon = 1 \rightarrow \Delta LWup = 1.22 Watt/m^2$

According to our error budget, neither the threshold requirement for accuracy nor that for precision is met. Since VIIRS calibration and radiometric noise errors are not expected to introduce more than a 4 W m^{-2} accuracy error and 2 W m^{-2} precision error, respectively (see Tables 6 and 7), this failure to meet threshold requirements is mostly attributable to error in other VIIRS EDRs or non-VIIRS data.

The main error on net heat flux EDR is resulted from the uncertainty of non-VIIRS data. It fails to meet the threshold requirements for precision and accuracy when the uncertainty of non-

VIIRS data is considered. The error budget is analyzed item-by-item below, and compiled in Tables 6-7.

a. Forward model

MODTRAN 3.7 is used to calculate the long-wave net radiation flux at the surface. 6S is applied to calculate the short-wave radiation flux at the surface. It is generally believed that an error of 5 Wm^{-2} may exist in the measurements by using pyranometers for global radiation and pyrgeometers for the long-wave radiation flux. Thus, the 5 Wm^{-2} has been chosen here as the accuracy error in either forward model or in the measurement.

b. Atmospheric correction

A multiple regression method is used to calculate the downward short-wave radiation flux from VIIRS measurements. The scatter in this regression is used to derive an atmospheric correction error of 3.5 Wm^{-2}.

c. Sea surface wind speed

The sea surface wind speed is required for calculating the sensible and latent heat fluxes and the sea surface albedo required for the computation of net shortwave flux. The NPOESS CMIS instrument will provide both the sea surface wind speed and direction. The wind speed product of CMIS is required to have the accuracy of 1m/s or 10% of the true value, whichever is greater (NPOESS CMIS SRD requirement). The uncertainty of the sea surface wind speed can result in an error of approximately 8 Wm^{-2}. The wind direction is not considered in the bulk formula.

d. Temperature profile

The temperature profile is an important parameter for calculating the downward long-wave radiation flux at the surface. The uncertainty of the temperature profile is 1 K for the layer between the surface and 300 hPa (NPOESS CrIS SRD threshold requirement). The atmospheric effect on the downward long-wave radiation above 300 mb is small. The uncertainty of 1 K in the error budget has been adopted. The uncertainty of the temperature profile can result in an error of approximately 3 Wm^{-2}. For the short-wave radiation flux at the surface, it has little effect.

e. Humidity profile

The humidity profile is an important parameter for calculating the downward long-wave and the short-wave radiation fluxes at the surface. The uncertainty for the humidity profile is 15% for the layer between the surface and 600 mb (NPOESS CrIS SRD threshold requirement). This uncertainty has been adopted in the error budget. The uncertainty of the humidity profile can result in a total error of approximately 8 $Wm^{-2}$for the short-wave and long-wave radiation flux at the surface.

f. Air temperature at surface

An uncertainty of 1 K for the surface air temperature is used. This is the same for the temperature profile. The air temperature effects the calculation of the sensible heat flux. The uncertainty of 1 K can result in an error of 6 Wm^{-2} for the net heat flux EDR.

g. Total column ozone

The total column ozone can be obtained from the operational product of OMPS, one of the NPOESS instruments. The ozone product is supposed to be better than 10 Dobson units (3 DU +/- 0.5%, NPOESS OMPS SRD). An uncertainty of 15 Dobson units is required. The error due to the uncertainty of the ozone amount is approximately 1 Wm^{-2}. The error in the ozone correction is used for all the error budget tables.

h. Surface specific humidity

The surface specific humidity is not available from NPOESS EDRs. It can be obtained by interpolating the humidity profile from CrIS or NCEP or from the surface temperature by assuming that the atmosphere just above the water or ice surface is saturated. The uncertainty of the surface specific humidity is too large compared to the VIIRS SRD requirement. Research results (Chou et al., 1995) have shown that the uncertainty can be as high as 2g/kg. The latent heat flux error is expected to be approximately 20 W/m^2 (Liu et al. 1999), which corresponds approximately to an uncertainty of 1 g/kg for the surface specific humidity.

i. Sea/ice surface temperature

The accuracy of 0.2 K for sea surface temperature can result in an error in the longwave, sensible, and latent heat fluxes of approximately 4.7 W/m^2 because the surface temperature affects the long-wave net radiation flux at the surface and the sensible and latent heat fluxes. The uncertainty of 0.3 K (Raytheon specified value) for ice surface temperature can result in an error approximately 4.9 Wm^{-2}.

j. Ice cover fraction

Near the water/ ice margin, an error in the estimate of ice cover fraction can result in an error

$$\Delta SW_{net} = \Delta f \cdot (\alpha_i - \alpha_w) \cdot SW_d$$

where ΔSW_{net} is the estimated error in the net downward shortwave flux, Δf is the error in the ice fraction, α_i is the albedo of ice, α_w is the albedo of water, and SW_d is the downward shortwave flux. Assuming values of 10% for Δf, 0.7 for a_i, 0.1 for a_w, and 200 W m^{-2} for SW_d yields a value of 12 W m^{-2} for ΔSWnet. The 10% value for Δf is equal to the uncertainty requirement for the VIIRS Ice Concentration ARP, but since the Net Heat Flux EDR is aggregated to a 20 km grid while ice concentration is given for each imagery-resolution pixel, with pixel size ~500m. This source of error has the potential to be highly variable, depending on the intensity of incoming shortwave radiation and ice albedo variation.

k. Absolute calibration

The surface short-wave radiation flux is almost linearly proportional to the calibrated radiance. Comparisons of the radiation budget at the top of the atmosphere between the VIIRS-derived and those obtained by other satellite-based sensors should be very helpful. The calibration stability for the VIIRS bands is more important than the absolute calibration because the calculated shortwave radiation flux can be recalibrated by the surface measurement (there are some operational stations for this measurement). We use 0.5% accuracy for the recalibration based on the current accuracy of the surface measurements The 0.5% calibration error can result in an error of 4 Wm^{-2} for the net heat flux EDR over the oceans for downward short-wave radiation flux at surface of 800 Wm^{-2} and 1.5 Wm^{-2} for downward short-wave radiation flux over ice of 300 Wm^{-2} (monthly mean value in polar summer).

l. Radiometric noise

The net heat flux EDR is not sensitive to the VIIRS radiometric noise. The high signal-to-noise ratio of the ocean color bands is sufficient for this EDR. The noise is assumed to have a Gaussian distribution. The error in the calculation of the net heat flux EDR due to the radiometric noise is less than 2 Wm^{-2} even without considering the aggregation of the pixels. The radiometric noise is negligible when one aggregates the VIIRS pixel into the 20 km by 20 km grid.

Table 6. VIIRS Net Heat Flux error budget – ocean case

Net Heat Flux	Case:	Ocean	Net SW Radiation Error			Net LW Radiation Error			Sensible Radiation Error			Latent Radiation Error			Total Error		
	Reference	Magnitude	Acc. W/m^2	Prec. W/m^2	Unc. W/m^2	Acc. W/m^2	Prec. W/m^2	Unc. W/m^2	Acc. W/m^2	Prec. W/m^2	Unc. W/m^2	Acc. W/m^2	Prec. W/m^2	Unc. W/m^2	Acc. W/m^2	Prec. W/m^2	Unc. W/m^2
System Specification															10.0	25.0	
System Performance															8.0	24.3	
Algorithm Performance			5.0	6.2	8.0	1.2	6.9	7.0	2.0	7.2	7.4	4.1	21.2	21.6	6.9	24.2	25.2
Forward Model	6S or MODTRAN	5 W/m^2	5.0	0.0	5.0	---	---	---	---	---	---	---	---	---	5.0	0.0	5.0
Atmospheric Correction	Regression	2 W/m^2	0.0	3.5	3.5	---	---	---	---	---	---	---	---	---	0.0	3.5	3.5
Surface Wind Speed	CMIS	10%	---	---	---	---	---	---	0.0	3.9	3.9	0.0	7.0	7.0	0.0	8.0	8.0
Temperature Profile	CRIS	1K	---	---	---	0.0	3.1	3.1	---	---	---	---	---	---	0.0	3.1	3.1
Humidity Profile	CRIS	15%	---	5.0	5.0	0.0	6.2	6.2	---	---	---	---	---	---	0.0	8.0	8.0
Air Temperature	CRIS	1K	---	---	---	---	---	---	0.0	6.0	6.0	---	---	---	0.0	6.0	6.0
Surface Specific Humidity	VIIRS SST	2 g/kg	---	---	---	---	---	---	---	---	---	0.0	20.0	20.0	0.0	20.0	20.0
Total Column Ozone	OMPS	10 DU	0.0	1.0	1.0	---	---	---	---	---	---	---	---	---	0.0	1.0	1.0
Sea Surface Temperature	VIIRS	0.3 K	---	---	---	1.2	---	1.2	2.0	0.0	2.0	4.1	0.0	4.1	4.7	0.0	4.7
Sensor Performance			4.0	2.0	4.5	---	---	---	---	---	---	---	---	---	4.0	2.0	4.5
Absolute Calibration		0.50%	4.0	0.0	4.0	---	---	---	---	---	---	---	---	---	4.0	0.0	4.0
Radiometric Noise			0.0	2.0	2.0	---	---	---	---	---	---	---	---	---	0.0	2.0	2.0

Acc. = accuracy Prec. = precision Unc. = uncertainty --- indicates that a source of error is not relevant to a NHF component

Table 7. VIIRS Net Heat Flux error budget – ice case

Net Heat Flux	Case:	Ice	Net SW Radiation Error			Net LW Radiation Error			Sensible Radiation Error			Latent Radiation Error			Total Error		
	Reference	Magnitude	Acc. W/m^2	Prec. W/m^2	Unc. W/m^2	Acc. W/m^2	Prec. W/m^2	Unc. W/m^2	Acc. W/m^2	Prec. W/m^2	Unc. W/m^2	Acc. W/m^2	Prec. W/m^2	Unc. W/m^2	Acc. W/m^2	Prec. W/m^2	Unc. W/m^2
System Specification															15	25	
System Performance															11.5	24.1	
Algorithm Performance			10.3	5.6	11.7	1.4	6.8	7.0	2.3	7.2	7.5	4.1	21.2	21.6	11.4	24.0	26.6
Forward Model	6S or MODTRAN	5 W/m^2	5.0	0.0	5.0	---	---	---	---	---	---	---	---	---	5.0	0.0	5.0
Atmospheric Correction	Regression	2 W/m^2	0.0	2.0	2.0	---	---	---	---	---	---	---	---	---	0.0	2.0	2.0
Surface Wind Speed	CMIS	10%	---	---	---	---	---	---	0.0	3.9	3.9	0.0	7.0	7.0	0.0	8.0	8.0
Temperature Profile	CRIS	1K	---	---	---	0.0	3.1	3.1	---	---	---	---	---	---	0.0	3.1	3.1
Humidity Profile	CRIS	15%	0.0	5.1	5.1	0.0	6.1	6.1	---	---	---	---	---	---	0.0	8.0	8.0
Air Temperature	CRIS	1K	---	---	---	---	---	---	---	6.0	6.0	---	---	---	0.0	6.0	6.0
Surface Specific Humidity	VIIRS SST	2 g/kg	---	---	---	---	---	---	---	---	---	0.0	20.0	20.0	0.0	20.0	20.0
Total Column Ozone	OMPS	10 DU	0.0	1.0	1.0	---	---	---	---	---	---	---	---	---	0.0	1.0	1.0
Ice Surface Albedo	VIIRS	3%	9.0	0.0	9.0	---	---	---	---	---	---	---	---	---	9.0	0.0	9.0
Ice Surface Temperature	VIIRS	0.3 K	---	---	---	1.4	0.0	1.4	2.3	0.0	2.3	4.1	0.0	4.1	4.9	0.0	4.9
Sensor Performance			1.5	2.0	2.5	---	---	---	---	---	---	---	---	---	1.5	2.0	2.5
Absolute Calibration		0.50%	1.5	0.0	1.5	---	---	---	---	---	---	---	---	---	1.5	0.0	1.5
Radiometric Noise			0.0	2.0	2.0	---	---	---	---	---	---	---	---	---	0.0	2.0	2.0

Acc. = accuracy Prec. = precision Unc. = uncertainty --- indicates that a source of error is not relevant to a NHF component

Even if the objectives for the atmospheric temperature and humidity profile EDRs can be achieved, large uncertainties remain for the latent and sensible heat fluxes. This point can be directly seen from the bulk formula, which indicates that ten percent error in the sea surface wind results in an error of 10 Wm^{-2} for the latent heat flux and an error of 3 Wm^{-2} for the sensible heat flux. A ten percent error in surface humidity results in errors of 15 Wm^{-2} and 8.4 Wm^{-2} for the latent and sensible heat fluxes, respectively.

The estimate of the total error for NHF EDR is about 26 Wm^{-2}. The estimated total accuracy and precision values are within the derived specifications shown in Table 1, but do not meet the threshold values.

3.4 ALGORITHM SENSITIVITY STUDIES

As shown in Figure 8, the downwelling shortwave radiation flux at the surface can be determined directly from VIIRS radiances. The longwave net radiation flux over oceans can be derived from CrIS or NCEP profiles and VIIRS SSTs. Both derived shortwave and longwave radiation flux accuracy errors are well below the value of the NPOESS threshold requirement for NHF accuracy in the ocean case. (Ice albedo accuracy error increases the contribution of shortwave radiation uncertainty to the NHF uncertainty in the ice case.) Shortwave and longwave precision errors each individually exceed the NPOESS threshold requirement for NHF. Expected uncertainties in surface and air temperature, specific humidity, and surface wind speed are too high for retrieved latent and sensible heat fluxes to have precision errors below the NHF threshold value.

3.4.1 Calibration Errors

The calibration request from the Net Heat Flux EDR is too high to be satisfied. A one percent calibration error in the shortwave region can cause an error of 10 Wm^{-2}. Therefore, the retrieved radiation fluxes over oceans need to be compared and adjusted with ground truth measurements, which can be obtained from BSRN (Baseline Surface Radiation Network). BSRN is a project of the World Climate Research Program (WCRP), aimed at detecting important changes in the earth's radiation field, which may cause climate changes. At a small number of stations (fewer than 40) in contrasting climate zones, covering a latitude range from 80°N to 90°S, solar and atmospheric radiation is measured with instruments of the highest available accuracy and at a very high frequency (minutes).

3.4.2 Instrument Noise

Only one of the four components—the shortwave radiation flux over the ocean surface—depends directly on the sensor noise. It can be seen from Figure 6 that sensor noise model 3 or better can satisfy the EDR requirement for precision. The actual VIIRS sensor noise is expected to be less noisy than sensor model 3.

3.4.3 Other

The VIIRS Net Heat Flux EDR is strongly dependent on the retrieval accuracy of other EDRs from VIIRS and other instruments (CrIS and CMIS) or meteorological analyses (NCEP). As is shown in the error analysis above, we do not expect these data to be provided at sufficient levels of accuracy and precision to meet the NHF threshold requirements, but we do expect to be able to meet specifications. Figures 11 and 12 show estimates of the sensitivity of sensible and latent heat flux to variation in the uncertainty of sea surface temperature and surface wind speed, two key parameters in the derivation of those fluxes.

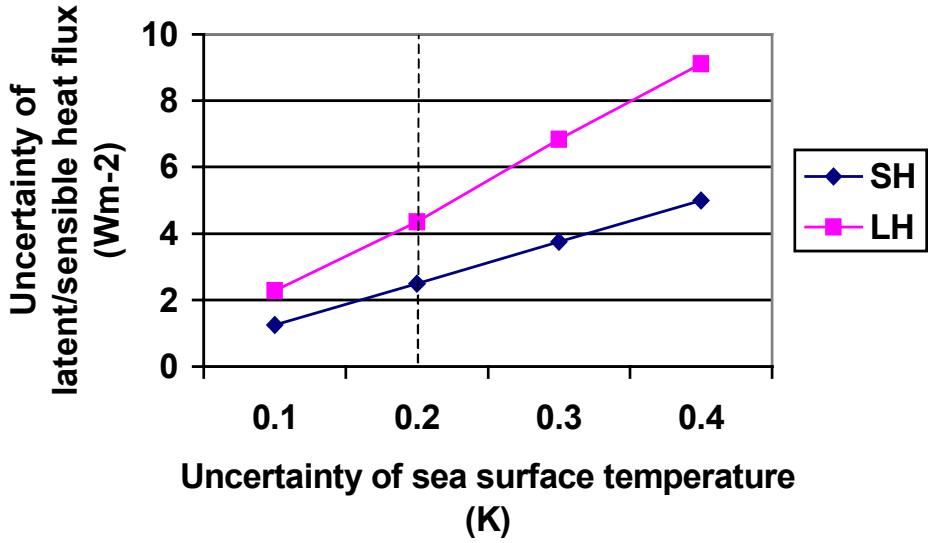

Figure 11. Sensitivity test for the latent and sensible heat fluxes with the uncertainty of the sea surface temperature. Dashed line shows the anticipated sea surface temperature uncertainty.

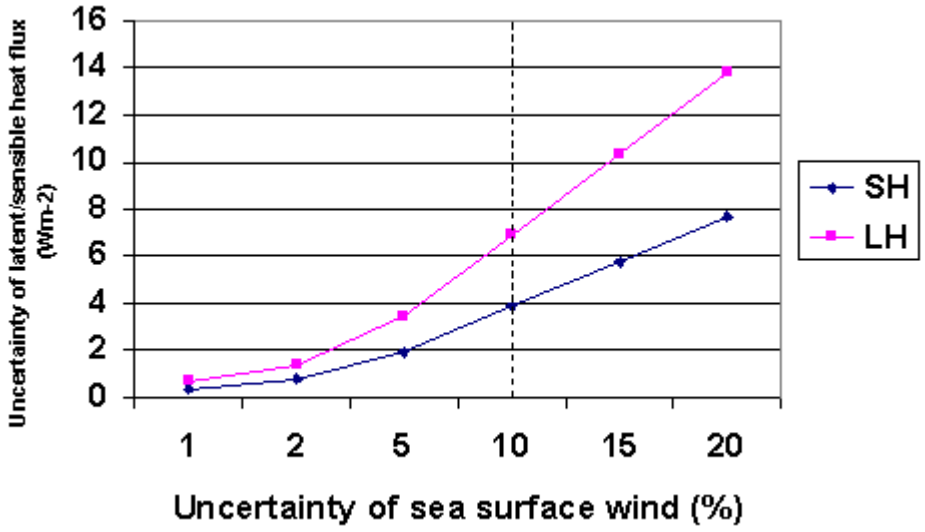

Figure 12. Sensitivity test for the latent and sensible heat fluxes with the uncertainty of the sea surface wind speed. Dashed line shows the anticipated sea surface wind speed uncertainty.

3.5 PRACTICAL CONSIDERATIONS

Net Heat Flux retrievals could be improved via aggregation or through improvements to the retrievals of other VIIRS EDRs or auxiliary data. As an example of the effects of aggregation, the uncertainty of the sea surface temperature derived from the VIIRS instrument is better than 0.5 K for a spatial resolution of about 1.3 km. For a spatial resolution of 20 km, a threshold requirement of the Net Heat Flux EDR, a better precision of 0.3 K for the sea surface temperature can be expected.

3.5.1 Numerical Computation Considerations

Due to the necessity of looping over many pixels to perform each aggregation, it will be important to take measures to reduce algorithm run time.

3.5.2 Programming and Procedural Considerations

Algorithms could be developed for retrieving the difference between SST and air temperature and for the difference between humidity at skin and humidity at ten meters above the skin. Combining VIIRS and CrIS data, an improved retrieval algorithm for boundary layer conditions could be developed. All codes will be written in FORTRAN.

3.5.3 Configuration of Retrievals

The configuration of the retrieval for the Net Heat Flux is separated into parts: radiation fluxes and turbulent fluxes. Shortwave net radiation at the surface will be calculated from shortwave VIIRS radiances based on a regression method. Another method for calculating shortwave net radiation flux has been described by Darnell *et al*. (1992) The use of this method would require the VIIRS aerosol optical depth and CrIS atmospheric temperature and humidity profiles products, as well as from the total ozone amount by an empirical formula. This method has not been tested here, but represents a potential algorithm improvement. The longwave net radiation flux will be calculated from the atmospheric temperature and humidity profiles and sea or ice surface temperature by applying an empirical formula (Gupta *et al*. 1992). A retrieval package for the boundary layer has been developed for calculating the low- level air temperature and surface specific humidity from VIIRS and CrIS data. Using this package, the bulk coefficients needed for sensible and latent heat retrieval could be calculated from the boundary parameters: air temperature, sea surface temperature, surface specific humidity, and sea surface wind. However, it is not clear whether it will be possible to make such retrievals, which require combining data simultaneously taken by different NPOESS instruments.

3.5.4 Quality Assessment and Diagnostics

Because the Net Heat Flux is for the clear sky cases only, the local variation of the shortwave net radiation flux over oceans should be relatively small. In order to ensure that cloud contamination does not occur, the validity of the VIIRS cloud masking algorithm will need to be tested. The monthly mean value of the shortwave net radiation fluxes must be checked against the ground truth to allow calibration. Any large jump of ten percent (daily) from a previous day will be automatically checked to verify whether the large jump is due to volcanic ash or a calibration error. The variation of the longwave net radiation flux and the latent and sensible heat fluxes can be large in the neighborhood of baroclinic fronts.

3.5.5 Exception Handling

If CMIS is not available, the sea surface wind speed from SSM/I or analysis from a numerical model such as NCEP will be used. Atmospheric profiles of temperature and humidity are also required from an analysis if both CMIS and CrIS are not available.

3.6 ALGORITHM VALIDATION

The algorithm validation will be performed in two ways: model simulations and comparisons with other data sets, for example, ground measurements and other satellite measurements such as CERES (Clouds and the Earth's Radiation Energy System). Simulations will be performed using the commonly applied radiative transfer codes and radiosonde measurements. It is found the VIIRS radiances for the sensor model 3 or better can be used to determine the shortwave net radiation flux over the oceans (see Figure 6). The shortwave radiation fluxes at the top of the atmosphere can also be derived from VIIRS radiances (see Figure 13). The CrIS derived atmospheric profiles and VIIRS aerosol optical depth can be applied to calculate the radiation flux at the top of the atmosphere. A fast algorithm for calculating the downward longwave flux from the atmospheric profile has been developed and tested. The algorithm is based on the

results of empirical orthogonal function analysis. Figure 14 shows very good agreement between the results from detailed MODTRAN radiative transfer calculation and the present retrieval. One can compare the results with the measured fluxes at the top of the atmosphere from CERES to recalibrate the surface radiation fluxes derived from VIIRS. The turbulent energy can be checked with ground truths. Air temperature and surface humidity as well as sea surface wind can be compared with the values from a numerical prediction model or from surface-based measurements.

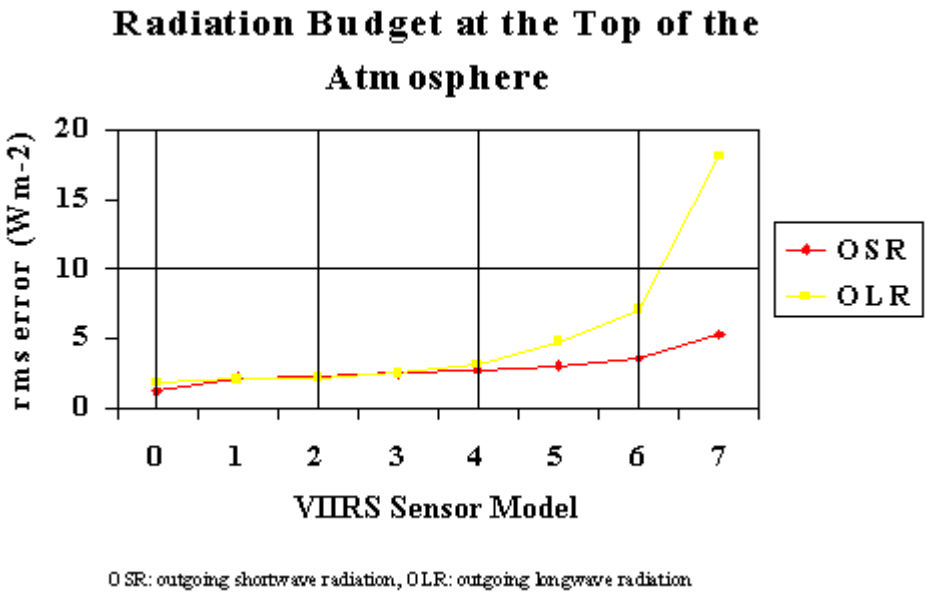

Figure 13. Retrieval errors for the radiation flux at the top of the atmosphere for different sensor models.

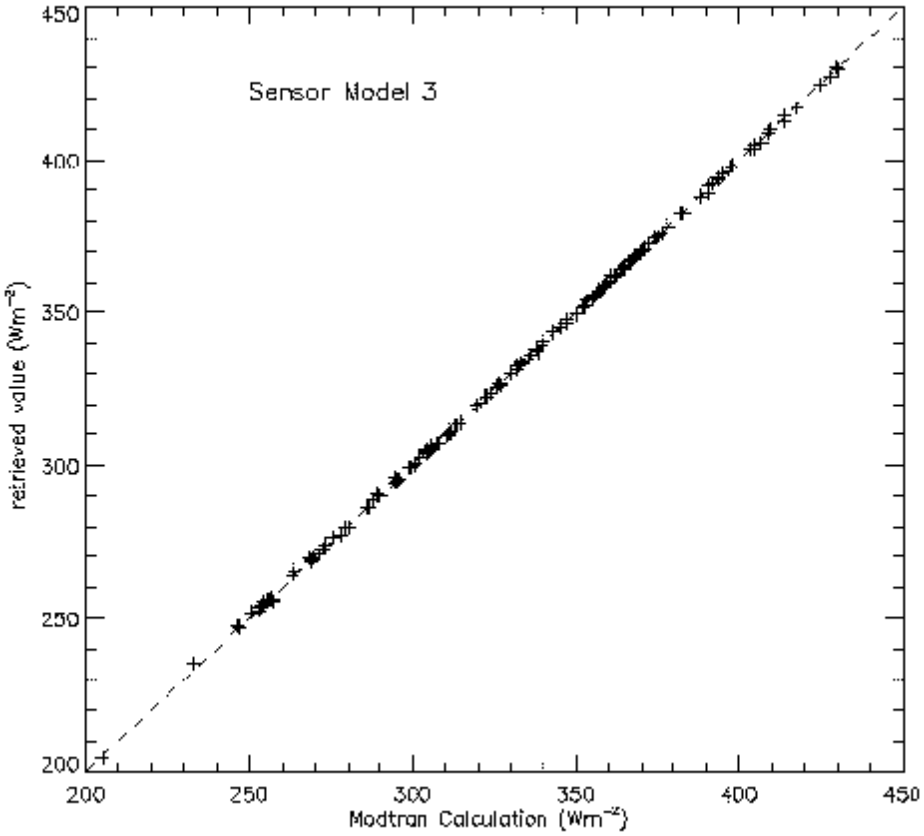

Figure 14. Comparisons of the downward surface longwave flux over the ocean between detailed MODTRAN calculations and present retrieval.

3.7 ALGORITHM DEVELOPMENT SCHEDULE

An algorithm for calculating downward surface shortwave radiation flux from VIIRS measurements has been developed. The algorithms for calculating the longwave net flux at surface and latent and sensible heat fluxes from atmospheric profiles have also been developed. However, the results do not meet the SRD thresholds for accuracy and precision due to the expected errors in other VIIRS EDRs and auxiliary data.

Algorithm tests show that downward short-wave radiation flux over oceans can be calculated accurately from VIIRS radiance (see Figure 15). For a given surface albedo of ice, the short-wave net radiation flux over ice also can be derived from VIIRS radiance (see Figure 16).

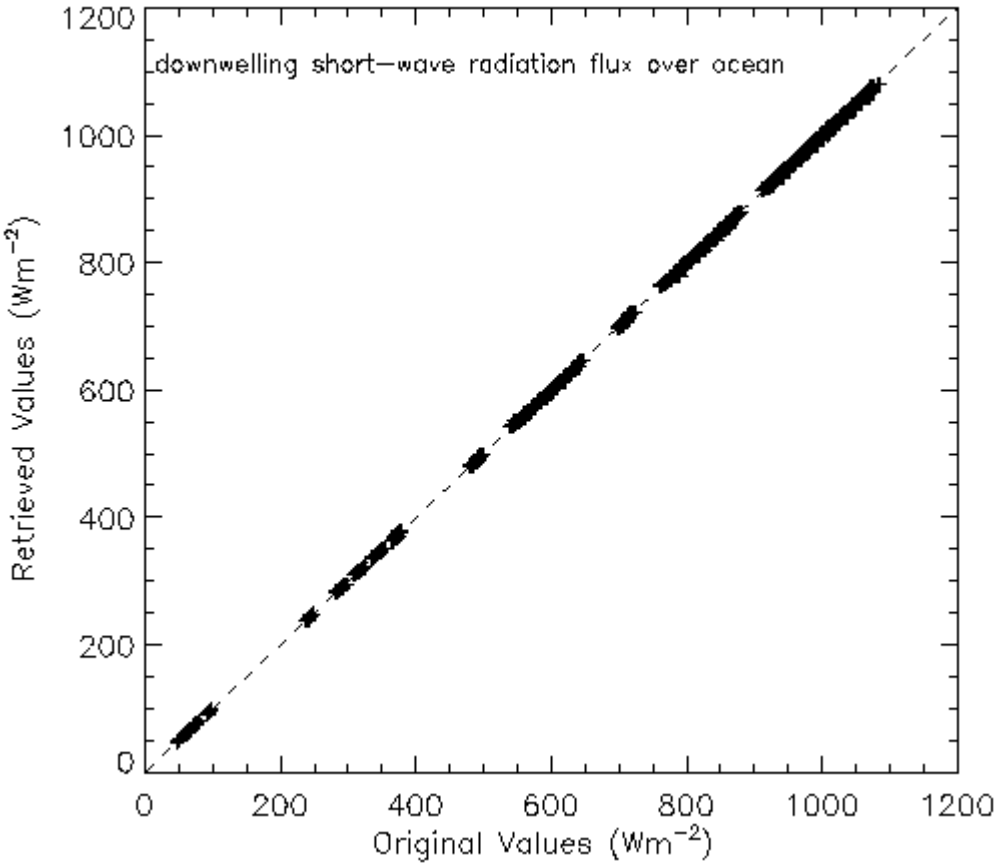

Figure 15. Comparisons of original and VIIRS radiance retrieved short-wave net radiation flux over the oceans.

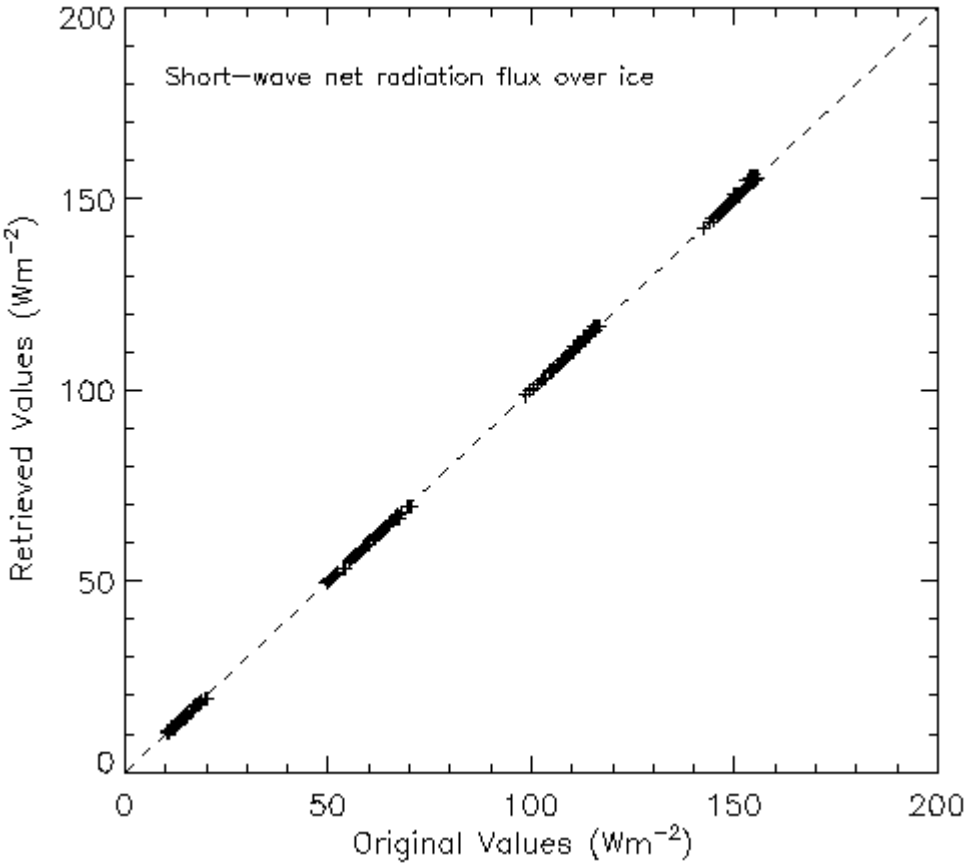

Figure 16. Comparisons of original and VIIRS radiance retrieved short-wave net radiation flux over ice.

4.0 ASSUMPTIONS AND LIMITATIONS

The primary assumptions and limitations of our methods are itemized here according to the component of the NHF EDR that they affect.

4.1 ASSUMPTIONS

Net Shortwave Radiation: The radiative transfer code MODTRAN is assumed to be within an accuracy of 5 Wm^{-2} for the calculation of the surface radiation fluxes (if a MODTRAN-based look-up table is used).

The ice albedo and ice fraction will be provided to the levels of accuracy and precision stated in our error budget (Section 3.3.4.3).

Net Longwave Radiation: The atmospheric temperature and humidity profiles and surface temperature data will be provided to the levels of accuracy and precision stated in our error budget (Section 3.3.4.3).

The Gupta *et al*. (1992) method for longwave flux retrieval is applicable in the conditions under which our retrievals are performed.

Sensible and Latent Heat: The atmospheric temperature and humidity profiles and surface temperature and wind speed data will be provided to the levels of accuracy and precision stated in our error budget (Section 3.3.4.3).

The bulk turbulent transfer formulae are applicable in the conditions under which our retrievals are performed and a proper selection of bulk transfer coefficients is made.

4.2 LIMITATIONS

Net Shortwave Radiation: Retrievals are limited to clear conditions where the sea surface wind is below 25 ms^{-1}, and to the range of atmospheric and surface conditions included in the shortwave regression coefficient look-up table.

Net Longwave Radiation, Sensible, and Latent Heat: In order to meet the threshold requirement for the precision of 5 Wm^{-2} the total uncertainty for both the sea surface temperature and air temperature must be less than 0.2 K. The uncertainty for surface specific humidity needs to be smaller than two percent. Presently, such high requirements for the air temperature and surface specific humidity should not be expected.

All NHF components: Due to the 20 km aggregation interval, retrievals are likely to be less accurate where atmospheric or surface conditions vary sharply within a small spatial range, such as near water-ice margins or baroclinic fronts. Sufficient clear and otherwise uncontaminated pixels must be present within a 20 km grid cell for aggregation to be performed without introducing large errors.

5.0 REFERENCES

5.1 VIIRS DOCUMENTS

[Y-1] Visible/Infrared Imager/Radiometer Suite (VIIRS) Sensor Requirements Document (SRD) for National Polar-orbiting Operational Environmental Satellite System (NPOESS) Spacecraft and Sensors, Version 3, June 2000.

[Y-2386] Visible/Infrared Imager/Radiometer Suite (VIIRS) Sea Surface Temperature Algorithm Theoretical Basis Document, Version 5, March 2002.

[Y-2466] Visible/Infrared Imager/Radiometer Suite (VIIRS) Imagery Algorithm Theoretical Basis Document, Version 5, March 2002.

[Y-3230] Visible/Infrared Imager/Radiometer Suite (VIIRS) Net Heat Flux Unit Level Detailed Design, Version 4, January 2002.

5.2 NON-VIIRS DOCUMENTS

Agee, E. M., and R. P. Howley (1977). Latent and sensible heat flux calculations at the air-sea interface during AMTEX 74, *J. Appl. Meteor*., 16, 443-447.

Anderson, E. R.(1952). Energy budget studies. *U.S. Geol. Surv. Circ*., 229, 71-119.

Berk, A., L.S. Bernstein, and D.C. Robertson, MODTRAN: A Moderate Resolution Model for LOWTRAN 7, Air Force Geophysics Laboratory Technical Report GL-TR-89-0122, Hanscom AFB, MA.

Blanc, T. V. (1987). Accuracy of bulk method determined flux, stability, and roughness, *J. Geophys. Res*., 29, 3867-3876.

Brutsaert, W. (1982). *Evaporation into the Atmosphere*. Kluwer, Dordrecht, Holland: Boston: Reidel: Hingham, MA., 299pp.

Budyko, M. I. (1974). Climate and Life. *Int. Geophys. Ser*., Vol. 18, Academic Press, London, 508 pp.

Chou, S.-H. (1993). A comparison of airborne eddy correlation and bulk aerodynamic methods for ocean-air turbulent fluxes during cold-air outbreaks. *Bound.-Layer Meteor*., 64, 75-100.

Chou, S.-H., R. M. Atlas, C. L. Shie, J. Ardizzone (1995). Estimates of surface humidity and latent heat fluxes over oceans from SSM/I data, *Monthly Weather Review*, 123, 2405-2425.

Curry J. A., C. A. Clayson, W. B. Rossow, R. Reeder, Y.-C. Zhang, P. J. Webster, G. Liu, and R.-S. Sheu, 1999: High-Resolution Satellite-Derived Dataset of the Surface Fluxes of Heat, Freshwater, and Momentum for the TOGA COARE IOP. *Bull. Ame. Meteorol. Soc*., 80, 2059-2080.

Darnell, W. L., W. F. Staylor, S. K. Gupta, N. A. Ritchey, and A. C. Wilber (1992). Seasonal variation of surface radiation budget derived from International Satellite Cloud Climatology Project C1 data. *J. Geophys. Res*., 97, 15741-15760.

Darnell, W. L., and W. F. Staylor (1988). Estimation of surface insolation using sun-synchronous satellite data. *J. Climate*, 1, 820-835.

Fung, I. Y., D. E. Harrison, and A. A. Lacis. (1984). On the variability of the net longwave radiation at the ocean surface. *Rev. Geophys*., 22, 177-193.

Garratt, J. R. (1977). Review of drag coefficients over oceans and continents. *Mon. Wea. Rev*., 105, 915-929.

Gilman, C. and C. Carrett (1994). Heat flux parameterizations for the Mediterranean Sea: The role of atmospheric aerosols and constraints from the water budget. *J. Geophys. Res*., 99, 5119-5134.

Graf, J. E., Wu-yang Tsi, and L. Jones (1998). Overview of QuikSCAT mission- a quick deployment of a high resolution, wide swath scanning scatterometer for ocean wind measurement. Proceedings, IEEE Sotheastcon 1998, "Engineering for a New Era". (Cat. No. 98CH36170), p. xiv+416, 314-17.

Gupta, S. K. (1989). A parameterization for longwave surface radiation from sun-synchronous satellite data, *J. Climate*, 2, 305-320.

Gupta, S. K., W. L. Darnell, and A. C. Wilber (1992). A parameterization for longwave surface radiation from satellite data – Recent improvements, *J. Appl. Meteorol*., 31, 12, 1361-1367.

Haferman, J. L., E. N. Anagnostou, D. Tsintikidis, W. F. Krajewski, and T. F. Smith (1996). Physical based satellite retrieval of precipitation using a 3 D passive microwave radiative transfer model. *J. Atmos. Oceanic Technol*., 13, 832-850.

Hansen, J. E., G. Russel, D. Rind, P. Stone, A. Lacis, L. Travis, S. Lebedeff, and R. Ruedy, (1983). Efficient three-dimensional global models for climate studies: Model I and II. *Mon. Wea. Rev.*, 111, 609-662.

Harris, A. R., S. J. Brown, and I. M. Mason (1994). The effect of wind speed on sea surface temperature retrieval from space. *Geophy. Res. Lett*., 21, 1715-1718.

Hennings, D., M. Quante, and R. Sefzig (1990). International Cirrus Experiment 1989 Field Phase Report. *Institute of Geophysics und Meteorology*, University of Köln, F. R. Germany, 129 pp.

Isemer, H-J. and L. Hasse (1985). The Bunker Climate Atlas of the North Atlantic Ocean. Vol. 1, *Observations*. Spinger Verlag, Berlin, 218 pp.

Karstens, U., C. Simmer, and E. Ruprecht (1994). Remote sensing of cloud liquid water. *Meteorol. Atmosph. Phys*., 54, 157-171.

Kondo, J. (1975). Air-sea bulk transfer coefficients in adiabatic conditions. *Boundary Layer Meteorol*., 9, 91-112.

Large, W. G., and S. Pond (1981). Open ocean momentum flux measurements in moderate to strong winds, *J. Phys. Oceanogr*., 12, 464-482.

Li, Z., H. G. Leighton, and R. D. Cess (1993). Surface net solar radiation estimated from satellite measurements – comparisons with tower observations. *J. Climate*, 6, 1764-1772.

Liebe, H. J. (1985). An updated model for millimeter wave propagation in moist air. *Radio Science*, 20, 1069-1089.

Liou, K. N. (1986). Influence of cirrus clouds on weather and climate processes: A global perspective. *Mon. Wea. Rev*., 114, 1167-1199.

Liu, Q., and E. Ruprecht (1996). A radiative transfer model: matrix operator method. *Appli. Opt*., 35, 4229-4237.

Liu, Q., C. Simmer, and E. Ruprecht (1997). Estimating longwave net radiation at sea surface from the special sensor microwave/imager (SSM/I). *J. Appl. Meteorol*., 36, 919-930.

Liu, W. T., K. B. Katsaros, and J. A. Businger (1979). Bulk parameterization of air-sea exchanges of heat and water vapor including the molecular constraints at the surface. *J. Atmos. Sci*., 36, 1722-1735.

Liu, W. T. and A. Zhang (1994). Evaporation and solar irradiance as regulators of sea surface temperature in annual and interannual change. *J. Geophys. Res*., 99, 12623-12637.

Paulson, C. A., E. Leavitt, and R. G. Fleagle (1972). Air-sea transfer of momentum, heat and water determined from profile measurements during BOMEX. *J. Phys. Oceanogr*., 2, 487-497.

Priestley, C. H. B. (1966). The limitation of temperature by evaporation in hot climate. *Agric. Meteorol*., 3, 241-246.

Ramanathan, V. (1986). Scientific use of surface radiation budget data for climate studies. Position paper in NASA RP-1169.

Ramanathan, V. and W. Collins (1991). Thermodynamics regulation of ocean warming by cirrus clouds deduced from observations of 1987 El Nino. *Nature*, 351, 27-32.

Robinson, I. S., N. C. Wells, and H. Chamoch (1984). The sea surface thermal boundary layer and its relevance to measurement of sea surface temperature by air-borne and space-borne radiometers. *Int. J. Rem. Sens*., 5, 19-45.

Schluessel, P. (1996). Satellite remote sensing of evaporation over sea. NATO ASI Series, Vol. 45, Radiation and water in the climate system: 431-461.

Schmetz, J. (1986). An atmospheric-correction scheme for operational application to METEOSAT infrared measurements. *ESA*, 10, 145-159.

Schmetz, J. (1989). Towards a surface radiation climatology: Retrieval of downward irradiances from satellites. *Atmospheric Research*, 23, 287-321.

Simmer, C. (1994). Satellitenfernerkundung Hydrologischer Parameter der Atmosphäre mit Mikrowellen. Verlag, Dr. Kovac, 313 pp.

Smith, W. L. and H. M. Woolf (1983). Geostationary satellite sounder (VAS) observations of longwave radiation flux. Paper presented at the: Satellite Systems to Measure Radiation Budget Parameters and Climate Change Signal. International Radiation Commission, Igls, Austria, 29, Aug.–2 Sep.

Sorbjan, Z. (1989). Structure of the Atmospheric Boundary Layer. Englewood Cliffs, NJ: Prentice-Hall.

Vermote, E. F., J. L. Deuze′, M. Herman, and J. J. Morcrette (1997). Second simulation of the satellite signal in the solar spectrum GS: Overview. *IEEE Trans. Geosci. and Remote Sensing*, 35, 675-686.

Wisler, M. M. and J. P. Hollinger (1977). Estimation of marine environmental parameters using microwave radiometric remote sensing systems. N.R.L. Memo. Rept. 3661, pp 27.

Zhi, H. and Harshvardhan (1993). A Hybrid Technique for Computing the Monthly Mean Net Longwave Surface Radiation over Oceanic Areas. *Theor. Appl. Climatol*. 47, 65-79.